1973

A reverse flow boiling thermosiphon loop : design and feasibility study.

Robert G. S. Gaspar
University of Windsor

A REVERSE FLOW, BOILING THERMOSIPHON LOOP

(Design and Feasibility Study)

A Thesis
Submitted to the Faculty of Graduate
Studies through the Department
of Mechanical Engineering in
Partial Fulfilment of the
Requirements for the Degree of
Master of Applied Science
at the
University of Windsor

by

Robert Gaspar

Windsor, Ontario

1973

ABSTRACT

An experimental study was undertaken to investigate some of the factors affecting the operation of a fixed geometry, two phase thermosiphon loop after first determining that such a system is capable of operation, if initiated, when there is no external pumping and the flow direction is opposite to that generated by natural convection. The loop was constructed of glass with an internally heated annular heat input section, using Freon 113 as the working fluid and having an overall fluid depth of 13.1 feet. The effect of additional pressure drops of various magnitudes created by orifice plates which could be inserted at several locations in the riser section and the effect of the heater length and its location on the limiting values of the system output quality, heat input and flow rate were studied. In addition photographic and visual observations were made of the boiling phenomena and flow regimes including the behaviour of the system before and during flow reversal.

The information gathered indicates that there are both maximum and minimum performance limits for this type of system, that it is a functional method of utilizing bouyancy forces to maintain an unnatural flow direction once it is generated and that it is possible to predict the loop performance using a simple mathematical model.

ACKNOWLEDGEMENTS

The author would like to thank Dr. T.W. McDonald for his supervision of the project, Mr. Helmut Keil for his assistance with some of the problems encountered, Mr. Otto Brudy and Mr. Reg Myers who provided aid in the construction of the equipment, Mrs. B. Carr for the typing of the thesis and the National Research Council for its financial assistance under grant in aid A0877.

TABLE OF CONTENTS

TABLE OF CONTENTS CONT'D.

LIST OF FIGURES

LIST OF FIGURES (CONT'D.)

LIST OF TABLES

NOMENCLATURE

A	flow area, ft^2
C_p	specific heat, Btu/lbm °R
D	diameter, ft
D_e	equivalent diameter, ft
f_F	Fanning friction factor
g	acceleration due to gravity, ft/sec^2
g_c	gravitational constant, $lbm \cdot ft/lbf \cdot sec^2$
G	mass flux density, $lbm/ft^2 \cdot hr$
Gr	Grashoff Number, $D^3 \rho^2 \beta \Delta t/\mu^2$
h	heat transfer coefficient, $Btu/ft^2 \cdot hr \cdot °F$
h_{fg}	enthalpy, Btu/lbm
k	thermal conductivity, $Btu \cdot ft/ft^2 \cdot hr \cdot °F$
K	friction loss coefficient
Ka	Von Karman Number, $f\ f_F\ (Re)^2$
L	length, ft
L_T	depth of working fluid in the system, ft
L_H	heater length, ft
$\dot{m}$	mass flow rate, lbm/sec
N	weighting factor
N_{Fr}	Froude Number, $V/\sqrt{g\ D}$
N_{NU_D}	Nusselt Number based on diameter, $h\ D/k$
N_t	number of tubes
P	static pressure, lbf/ft^2

P_{BR}	static pressure at the bottom of the riser section, lbf/ft^2
P_{HI}	static pressure at the bottom of the heat input section, lbf/ft^2
$P_{reservoir}$	static pressure in the reservoir-condenser section, lbf/ft^2
q	rate of heat transfer, Btu/hr
$\dot{Q}$	Volume flow rate, ft^3/sec
Q_{in}	rate of heat transfer to the working fluid, Btu/hr
Re	Reynolds Number, ρ V D/μ
s	flow area, ft^2
t	temperature, °F
t_m	mean temperature, °F
T	temperature, °F
V	specific volume, ft^3/lbm
$\hat{V}$	velocity, ft/sec
W_c	critical mass flow rate, lbm/sec
X	system output quality
y	length of flashing column, ft
z	elevation, ft
α	void fraction
β	coefficient of bulk expansion, 1/°F
Δ	difference in quantity
λ	latent heat of vapourization, Btu/lbm
μ	viscosity, lbm/ft.sec

π	3.1416
ρ	density, lbm/ft^3

Subscripts

g	gaseous phase
in	quantity entering heat input section
L	liquid phase
out	quantity leaving heat input section
sat	saturated condition

Units

Btu	British Thermal Unit
°F	degrees Fahrenheit
ft	feet
hr	hour
lbf	pound force
lbm	pound mass
°R	degrees Rankin
sec	second

I INTRODUCTION

One of the major reasons for interest in the mechanism of reversed flow thermosiphoning is the number of Canadian nuclear reactors built with vertical fuel channels. The coolant flow in most of these reactors is upward. With this type of reactor, fueling is accomplished from above; i.e. the fueling machine sits on top of the reactor. This configuration introduces a number of design factors, such as:

1. Additional reinforcement of the reactor to support the weight of the fueling machine.
2. Design of the valve on the fueling port.
3. Fuel handling equipment.
4. Anchorage of the fuel string in the channel.
5. Necessity of coupling the fuel bundles with a common tie rod.
6. Coolant pumping.

In the case of a reactor operated with the coolant flowing downwards and the fueling done from below, the factors listed previously may either be simplified or eliminated, e.g. a tie-rod would be unnecessary which would permit the use of an additional fuel rod in each fuel bundle. Another factor worthy of consideration is the case of a pump failure and subsequent reactor shut down.

In this case the coolant pumping must not be discontinued once the reactor is shut down. This is due to the physics of the reactor which will continue to generate heat in the reactor for quite some time after shut down. Although this heat generation is only a small percentage of the maximum possible output of the reactor and it does diminish slowly with time, it still must be removed from the reactor by a flowing coolant.

In the summer of 1968 the author became involved with the problem of downward flow while working as a summer student for Atomic Energy of Canada Limited. At that time the problem posed was a simple one; will a closed loop thermosiphon continue to operate with downward flow over the heater section without providing some external driving force.

Several experiments, which terminated in failure; were conducted with a test loop built for a different testing program. Finally a small test loop designated as the Freon Micro-Loop was constructed and testing was carried out as reported in a short paper (1). The results of the testing showed that the loop would operate with reverse flow over the heater section with or without boiling although there was a good deal of flow instability for the case of boiling.

Upon entering graduate school the author submitted a research proposal to study the region of stability and operating characteristics of a reverse flow, boiling thermosiphon having previously obtained written permission from A.E.C.L. to continue the study initiated there.

The ultimate goal of the project was to investigate those factors which control the flow stability and evaporative efficiency of a reverse flow, boiling thermosiphon loop.

There are many factors which may influence the stability limits of operation of a reverse flow thermosiphon, such as:

1. Fluid properties
2. Loop geometry (height, component sizes, shape, etc.)
3. Heater length
4. Heater location
5. Heat flux variation (profile)
6. Inlet subcooling
7. Flow restrictions

From the experience gained at A.E.C.L. it was decided that to provide a versatile flow loop, the thermosiphon should be constructed from interchangeable components. Further, it was decided that the loop should be primarily constructed with glass to allow visual observations of flow within the thermosiphon loop and because of the glass that a non toxic, low latent heat of evaporation liquid with a saturation temperature slightly higher than ambient room temperature at atmospheric pressure be chosen as the working fluid. Refrigerant 113 was thus chosen since its fluid properties were quite suited to the design requirements and an economical supply was available.

The choice of a glass system did impose some restriction such as insertion of monitoring systems for temperature, pressure and flow rate; maximum operating pressure and available component sizes but it was deemed essential for flow visualization. In fact the experimenter's ability to see the flow provided the insight for design changes that made stable, boiling, reverse flow in the system possible. The glass construction also made photographic recording of the visual characteristics of the modes of flow available for study by other investigators.

This thesis deals with the design and construction of the thermosiphon loop and the effects of varying the heater length, heater position and the effect of insertion of orifice plates of various sizes in various locations in the riser section of the flow loop on the maximum and minimum power dissipation and system output quality for stable operation of the reverse flow, boiling thermosiphon loop shown in Figure 1. For these tests the orifice plates can be considered to represent valves, obstructions and other devices causing frictional pressure losses and the heater length and location tests can be considered as similar to the length and location of the nuclear fuel bundles in the reactor system.

These tests were conducted with one fluid, one fixed geometry and two constant inlet subcooling values, one for maximum performance and one for minimum performance.

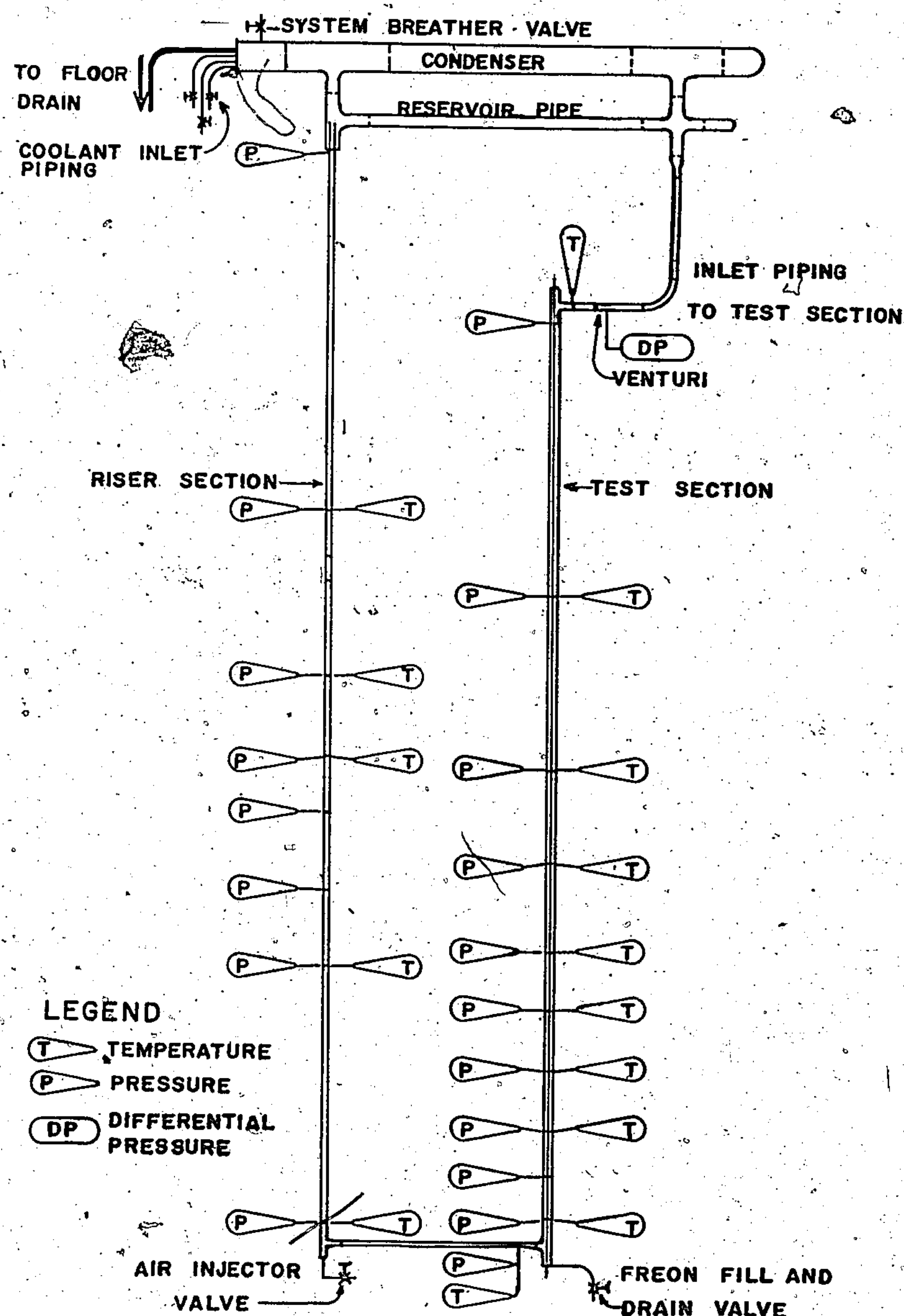

FIG. 1
DIAGRAM OF TEST APPARATUS

II LITERATURE SURVEY

The material in this chapter is included to provide information relevant to this problem and the references used in the analysis of the results obtained.

The idea of a boiling thermosiphon operating with the flow direction being opposite to the normal direction of natural convective flows cannot be attributed to any individual reference. Consequently and unfortunately there are few previous publications dealing with this problem. From information gathered at Atomic Energy of Canada Limited, from M.B. Carver, D.F. D'Arcy, G.A. Wikhammer and D.C. Groeneveld (2,3,4,5) and later from J.T. Rogers (6) indications were that reverse flow boiling thermosiphoning was being considered as a coolant flow mode for nuclear reactors in the case of cooling system pump failure when the nuclear chain heat reaction is interrupted and the reactor output diminishes to a small percentage of its maximum heat generation. The sources at AECL indicated that J.T. Rogers and G.M. Barns had completed some preliminary calculations indicating the feasability of this particular form of thermosiphoning. This work was followed up by R.G. Gaspar (author) who with the aid of D.C. Groeneveld constructed and tested a small thermosiphon loop (1). The report submitted by Gaspar indicated that reverse flow thermosiphoning was possible to achieve for both boiling and non-boiling cases.

A full report on the subject of reverse flow thermosiphoning was produced by G.M. Barns (see reference 7) which gave a literature survey and discussion of the problem as it pertains to nuclear reactors.

D.F. D'Arcy (8) suggested a 3:1 scaled down reactor loop that would be similar to one of the flow loops, U-1, in AECL's nuclear reactor NRU.

Other design ideas such as the use of glass piping for flow visualization and type of heating elements to provide power input were the result of experience gained by the author from another experimental study (9) conducted at AECL. The specific details (10) of a typical nineteen rod fuel bundle were used to determine a comparable hydraulic diameter for the annular flow passage heat input section of the test loop.

A venturi flow meter was designed employing design information outlined in an AECL Engineering manual (11) on that subject.

The condenser unit was designed according to established criteria outlined by both A.J. Chapman (12) and F. Kreith (13).

A Mechanical Engineering Laboratory manual (14) was the source of the procedure outline for calibrating the standard thermocouple used for the basic temperature measurements in the flow loop.

Data reduction and analysis were carried out by statistical methods outlined by A.M. Neville and J.B. Kennedy (15) with necessary supplementary information on the working fluid being provided by the ASHRAE Handbook of Fundamentals (16) and the Handbook of Tables for Applied Engineering Science (17).

From the references investigated several criteria for analysing the stability of the reverse flow direction were established. The first of these was found during the author's work at AECL.

An article on Sizing Piping for Process Plants (18) mentions a design problem encountered with two-phase vertical downward flow which may be applied to the analysis of stability for this problem. The author quotes several sources and establishes a value of Froude number modified for two phase flow as defined:

$$(N_{Fr})_L = \frac{\hat{V}_L}{\sqrt{gD}} \sqrt{\frac{\rho_L}{\rho_L - \rho_g}} \qquad \text{Eqn. 1}$$

where the lower limit of this number is given as 0.31 below which bubbles will not be swept downward by a downward flowing liquid.

Bonilla (19) states four criteria which may be used in flow loop design for downward flowing fluids and which may be helpful in establishing lower stability limits for the flow loop under investigation.

The first two criteria are based on pulsing which may develop in the flow if the flow rate is such that the flow switches from laminar to turbulent. This problem may be avoided if the Reynolds number and Von Karman number for the flow are outside the ranges indicated

$$2{,}100 < Re < 3{,}500$$

$$70{,}000 < Ka < 270{,}000$$

It is also noted that in annuli turbulence initiates less abruptly and pulsing is less likely to be encountered within this range.

One of the two other criteria given is the requirement that the ratio of the Grashoff number to Von Karman number be always much much less than unity ($Gr/Ka << 1$), see eqn. 2; where the Δt term in the Grashoff number is the temperature rise, not the wall to fluid temperature difference. Bonilla indicates that the reason for this limit is that an instability may develop under certain conditions so that a slight decrease in flow increases the bouyancy opposing flow and eventually leading to a flow reversal. The final criterion given is a critical flow value (see eqn. 3) below which flow reversal may be anticipated.

$$\frac{Gr}{Ka} = \frac{\rho^2 \, \beta g(t_2 - t_1) De}{4 \, f_F \, G^2} \qquad \text{Eqn. 2}$$

$$W_c = \left[\frac{\beta_1 \, g(t_2 - t_1) De}{8 \, f_F} \; \frac{\Delta z}{L} \right]^{1/2} \rho S \quad lbm/sec \qquad \text{Eqn. 3}$$

Information given by Pao (20) and Van Wylen and Sonntag (21) was used to evaluate the test data in light of the ideas presented in the two sources cited.

Other sources of information pertaining to this thesis may be found in the references listing (22,23).

III EXPERIMENTAL DETAILS

Introduction

In order to observe and measure the operating characteristics of a boiling reverse flow thermosiphon it was decided that the construction material of the system be glass. With this in mind it was therefore necessary to operate the system close to room temperatures to minimize heat losses so that insulation would not be required. This choice dictated that a working fluid be chosen which has a low saturation temperature at atmospheric pressure since low pressure operation was considered essential for reasons of operator safety.

A. Selection of Working Fluid

As indicated, the choice of the working fluid was influenced by the desire to be able to observe the fluid flow in the glass system and, because of this choice; the loop should operate at atmospheric pressure and near room temperature.

Originally Refrigerant 11 was considered as the working fluid primarily because of its common use as a working fluid at A.E.C.L. and because there is information available for comparison of R-11 and water. However, at the time when the project was initiated there was no temperature control for the laboratory room temperature during the summer months and on very hot days outside,the room temperature sometimes reached 85°F. Consequently R-11 was not used since its boiling point at atmospheric pressure is 74.7°F and under the room conditions mentioned the working fluid would require cooling to keep it in its liquid form. Also under the mentioned conditions it was envisioned that problems would be encountered with maintenance of liquid temperatures in the reservoir section which would increase the problem of controlling heat input during start up. In addition, even considering favourable room temperatures below the saturation temperature of R-11 there would be very little heat input needed to produce boiling in the heat input section.

Consequently, Refrigerant 113 (Trichlorotrifluoroethane) was chosen, based on its low saturation temperature of 117.6°F at atmospheric pressure, the fact that it remains a liquid even at elevated room temperatures, its low latent heat of vapourization, its low toxicity and its relatively low cost per pound.

B. Equipment and Design

1. Condenser Design

An arbitrary decision was made to build rather than purchase a condenser for the thermosiphon loop. The major factor influencing this decision was the consideration of problems arising from interfacing glass and metal parts such as allowing for different coefficients of thermal expansion, sealing of joints and problems of locating a suitable condensing heat exchanger. The selection of a glass encased condensing unit conquered most of these difficulties and left only the selection of a large enough size of glass pipe to contain the condenser tube arrangement designed.

The condenser capacity was determined by the electrical energy available at the test site which was 25 kilowatts. This figure was arrived at from the 240 volt, 100 ampere service available plus an anticipated use of a 1000 watt heating tape for auxiliary heating.

The estimated maximum cooling water inlet temperature selected was 80°F for mid-summer operation. The maximum operating pressure of 7.5 psig was determined to be a safe pressure limit assuming that the system might be pressurised for some test runs much later in the testing program. For the maximum pressure assumed, the maximum vapour temperature in the condenser would be 140°F. The maximum temperature rise of the cooling water was arbitrarily assumed to be 15°F.

With a general idea of what the final condenser unit would look like, several design requirements were determined. The first parameter was condenser tube diameter. From the three readily available sizes, 3/8 inch O.D. soft copper tubing was selected since the coolant flow area in a 1/4 inch O.D. tube is quite small and 1/2 inch O.D. tubing would be hard to work compared to 3/8 inch O.D. soft copper.

Having selected the condenser tube diameter and visualizing horizontal array of condenser tubes it was then necessary to determine the number of tubes per bank. This value was chosen to be 6 tubes per bank after considering the proposed geometry of the headers and since no great deviation from that number was considered likely and any deviation about it would not significantly affect other calculations.

The properties and conditions necessary for the condenser design are listed as follows:

$\Delta t = 140 - 95 = 45$ (assuming a maximum coolant temperature of 95°F)

$t_m = (140 + 95)/2 = 117.5°F$

$D = 3/8 \text{ inch} = 1/32 \text{ ft}$

$N_t = 6$

$g = 32.2 \text{ ft/sec}^2$

Evaluating the properties of saturated R-113 liquid at the mean film temperature

$\rho = 94.3 \text{ lb/ft}^3$

$\mu = 1.219 \text{ lb/ft-hr}$

$k = 0.034 \text{ Btu/hr-ft-°F}$

$\lambda = 61.3 \text{ Btu/lb}$

Substituting into eqn. 10.22 of Chapman (Eqn. 4)

$$N_{NU_D} = -.725 \left(\frac{g\ \rho^2\ \lambda\ D^3}{N_t\ \mu\ k\ \Delta t}\right)^{1/4} \qquad \text{Eqn. 4}$$

Then

$$N_{NU_D} = 114.5$$

Thus

$$hD = k\ N_{NU_D} = 3.89 \text{ Btu/hr-ft-°F}$$

Since $q = \pi L h D \Delta t$ Eqn. 5

then the required length of tubing is

$$L = \frac{q}{\pi h D \Delta t} \qquad \text{Eqn. 6}$$

$\therefore L = 155$ ft

The condenser unit was visualized as having a U-type tube arrangement and no more than three banks of tubes. Also since the space available in the lab was about 8 feet long, it was decided that the length of each "U" condenser tube be 5 feet which allows 3 feet for support members and cooling water facilities.

This indicated a final choice of 180 ft of tubing, since the total number of tubes was selected as 18. This allowed the condenser design to be on the conservative side and seemed to be a convenient arrangement of condenser tubes.

The decision regarding the physical layout of the condenser unit dictated that the condenser glass shroud must accommodate 36 condenser tubes with at least an equal area of free space surrounding them. This resulted in the selection of a 4 inch inside diameter glass pipe for the condenser shroud. The final overall length of the condenser as it was built was 7 feet with the additional length being used for the inlet and outlet headers and the connections to the condenser tubes.

The general construction of the condenser tube bank was quite simple. A 3.75 in diameter template was used during assembly to ensure sufficient space for the tubes when they were finally inserted in the glass shroud. The tubes were separated from each other by 1/8 inch diameter copper wires which were soldered to individual tubes at 1 foot intervals to maintain horizontal spacing of tubes at the same elevation and to keep the tube layers separated vertically.

The header system consisted of three controlled flow inlet headers, one for each tube bank; and one main outlet header collecting the coolant return and directing it to the floor drain. Each end of each U-shaped condenser tube is connected to its appropriate header by an accommodating length (2 to 12 inches) of soft polyvinyl chloride tubing which is clamped over the end of the copper tubing. This plastic tubing was selected on the basis of information that polyvinyl chloride is unaffected by contact with R-113.

A leakage problem encountered when preliminary testing was started. The problem arose from an unanticipated effect of the Refrigerant on the tubing used for connecting the condenser tubes to the headers. As was noted polyvinyl chloride is one of three plastics which is unaffected by contact with R-113, the other two being nylon and polytetrafluoroethylene.

It was concluded therefore that the connecting tubing supplied was certainly not one of these three listed because the shrinkage was at least 20% and there was no flexibility compared to another piece of tubing not used in the R-113 atmosphere. The tubing shrank and hardened sufficiently to loosen at the clamped ends enough so that it eventually pulled free. This required replacing the original tubing with new polyvinyl chloride tubing. To help prevent any further leakage, Lepage's Plastic Rubber was applied at the joints on the water side of each clamped joint. The solution improved the situation but problems of leaks still occurred which were possibly because of the variations in the length of the connecting plastic tubing. Finally it was decided to pressurize the condenser with a continuous flow of cooling water and this has proven successful since no further leakage was observed.

2. <u>Selection of Flow Loop Design</u>

The limitations which governed the selection of the glass piping and other hardware for the flow loop are: the hydraulic radius of the heat input section, the flow area of the venturi in the inlet to the heat input section, the flow area of the heat input section and the flow area of the riser be approximately the same. An added requirement was that all of the glass piping, the copper heating tube of the heat input section and the heater cartridges be stock items which would require little or no alterations before installation.

The hydraulic radius of the heat input section which was used to help make the component selections is similar to that of a typical working nuclear reactor which is approximately 0.0659 inches. This criterion was used because several small test loop facilities have hydraulic radii in the same range and this would seem to be a useful reference for comparison of different flow loops in use. The venturi used to measure the mass flow rate was also a governing factor since small sizes are difficult to manufacture. In this case it was determined that the bore diameter be no smaller than 0.50 inches.

The method planned for circulation of the working fluid was the use of air injection at the base of the riser section which would create a flow of the working fluid in the required direction.

The maximum thermosiphon height was dictated by the maximum floor to ceiling height of 18 feet 4 inches available in the Mechanical Engineering laboratory. With these basic requirements set it was then necessary to design the component sections of the thermosiphon loop with dimensions as given in the following sections.

3. Heat Input Section

The selection of an annular flow passage heat input section was determined by the general size of the test loop and the type of studies to be made. In larger models an attempt would have been made to provide a heat input section similar to that of a typical working nuclear reactor, i.e. separate heating elements for simulation of individual fuel rods.

Because of the nature of the investigation it was not deemed advisable since flow visualization was a requirement of the testing so that flow reversals could be observed. Therefore to provide a similar condition and to allow flow visualization an annular flow passage with a hydraulic radius of approximately 0.0659 inches was designed. With consideration of other component sizes and the intended use of stock items an outer wall inside diameter of one inch was selected which allowed the use of Q.V.F. (Quick Visible Flow) nominal one inch inside diameter glass pipe.

This selection would require the inner wall of the annulus to be 0.736 inches. A copper tube of the required outside diameter is not commercially available. Therefore there were essentially three possible options to choose from. A commercial 0.750 inch O.D. copper tube could be turned down on a lathe to the required diameter, the heating elements could be inserted in the same copper tube and it could be passed through a draw die to bring it down to size or the 0.750 inch O.D. copper tube could be used and the system would have a hydraulic radius of 0.0625 inches for the annular flow passage. Eventually the third possibility was chosen because, of the other two possibilities, the first would be difficult to achieve because of the cumbersome nature of working with a twelve foot length of copper tube in a lathe and the second choice would mean that special heating elements would be required to slip inside the tube or else the test section would have to be diassembled to insert a multitude of separate heating tubes (practically one for each test conducted).

The inner surface of the heat input section was therefore chosen to be a twelve foot length of precision drawn seamless copper tubing with an outside diameter of 0.75 ± 0.001 inches and an inside diameter of 0.526 ± 0.001 inches. This type of tube was used for all testing of the thermosiphon loop.

The first attempts at achieving reverse flow were conducted with a thermocouple instrumented heating tube of precision drawn seamless copper tubing with four 0.11 inch wide slots cut into the outer heating surface and running the full length of the tube. These slots were located at equally spaced circumferential positions to carry surface temperature measuring thermocouple lead wires. The lead wires were embedded in an epoxy resin cement which filled the slots.

Unfortunately during the first attempts at achieving reverse flow, many flow reversals were encountered because of the short heaters and lack of nucleation sites in the riser. These reversals occurred while air was still being pumped into the system and the pressure of air in the fluid allowed the heater sheath temperatures to rise high enough to cause a breakdown of the bond between the epoxy and the copper tube thereby allowing the thermocouple lead wires to pop out of their slots. Therefore a non-instrumented precision drawn copper tube was used for the majority of the testing program until the damage to the instrument tube could be corrected and until such a time when the operating range of the thermosiphon loop could be located so that the problems of damaging reversals in flow direction could be avoided.

As was noted previously the outer glass pipe used in the heat input section had an inside diameter of one inch +0.01, -0.02 inches so that the equivalent diameter of the heat input section was 0.25 + 0.01, -0.02 inches. These glass pipe sections are made with flared ends which are joined by a three bolt iron clamping ring with a graphite impregnated asbestos insert used for cushioning the glass against high stresses caused by unequal bolt tension.

Nylon spacer rings (see Figure 2) were machined to fit the inside glass flare (see Figure 3) in order to provide a means of securing fluid temperatures and pressures in the heat input section.

Besides allowing insertion of thermocouple probes and static pressure taps some of the nylon rings were fitted with three screw holes which could be used for centering the heating tube by means of three alignment screws.

A glass to nylon seal was achieved by inserting deformable teflon sealing rings between the two materials thus reducing the bolt tension and stress on the glass pipe required to attain a dry seal.

The heat input section length from inlet to outlet centreline is 129.5 inches and is made up of the glass pipe section lengths listed in order from top to bottom in Table 1.

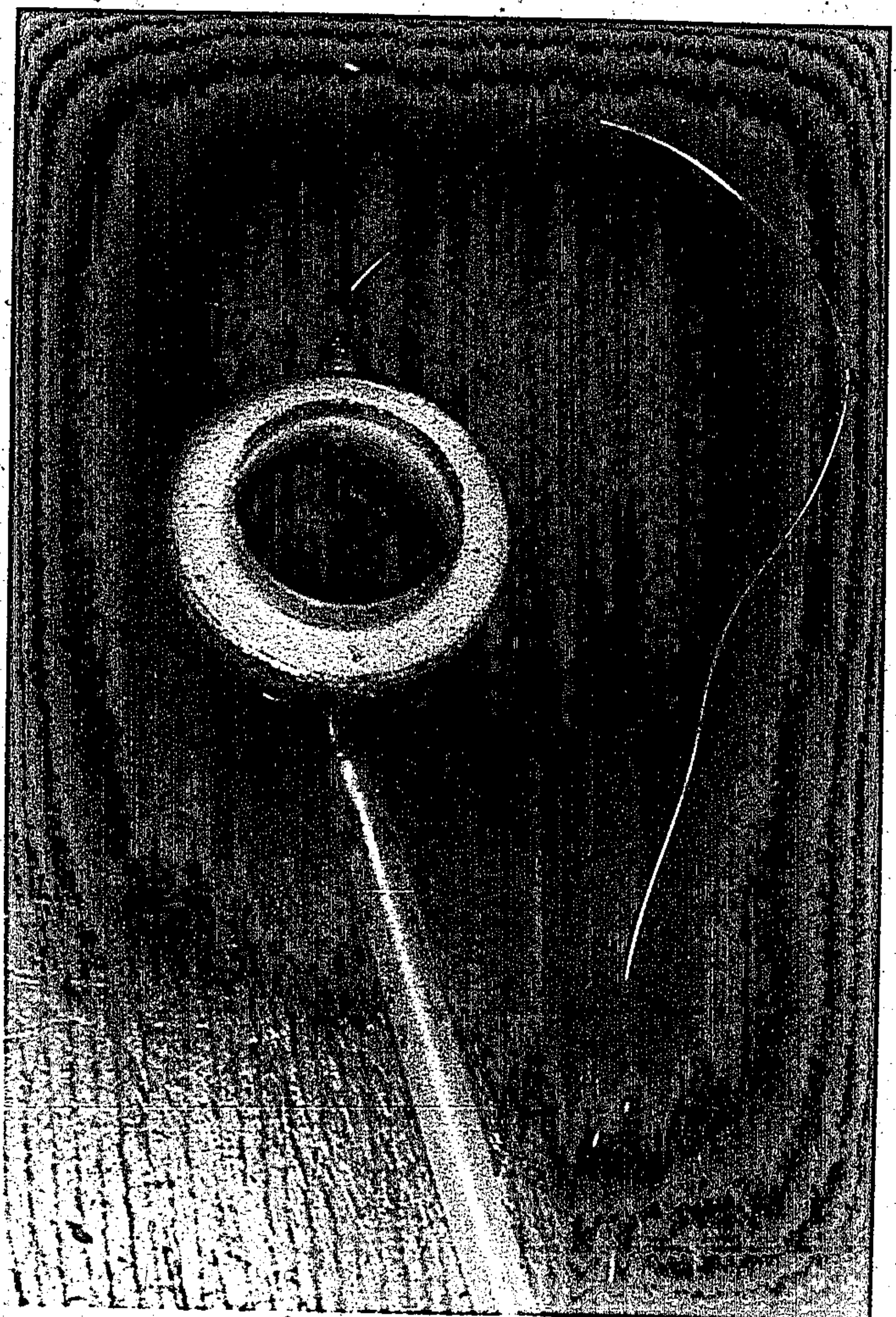

FIG. 2

NYLON INSERT RING OF HEAT INPUT SECTION

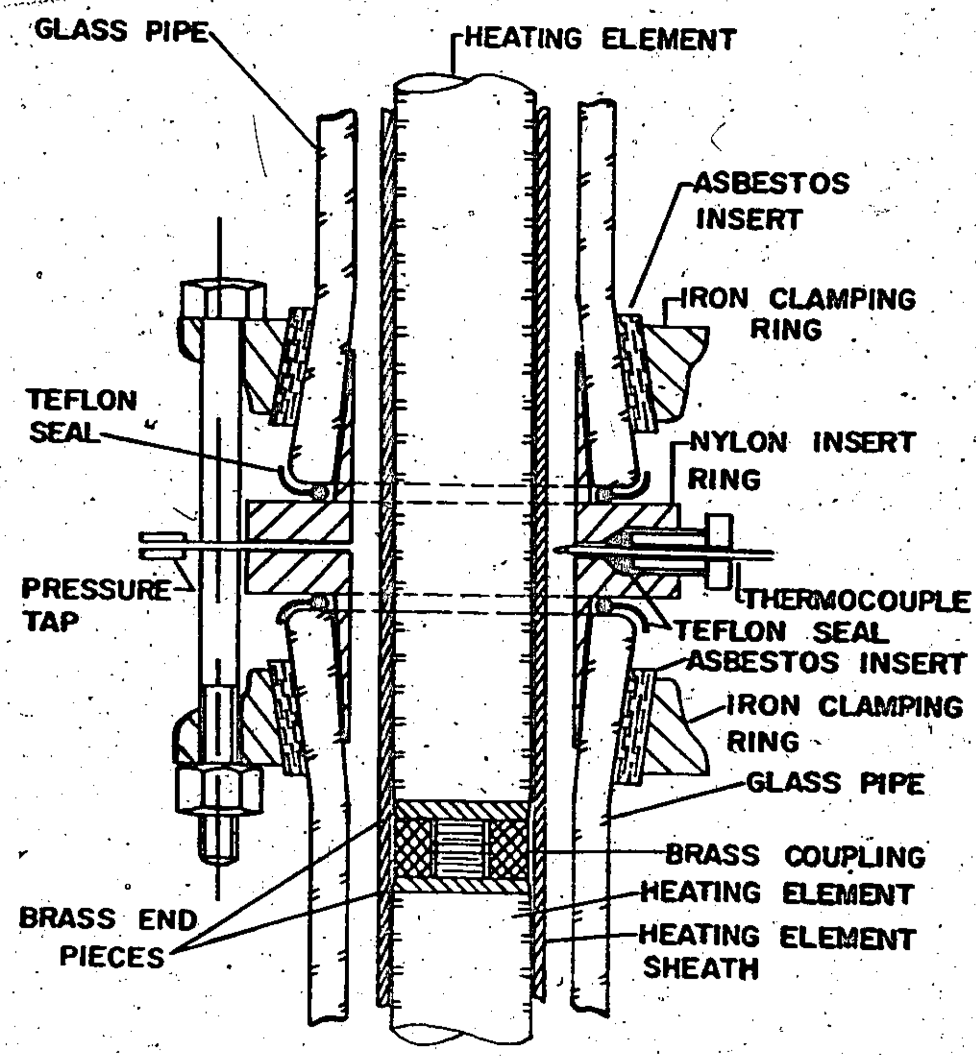

FIG. 3
DIAGRAM OF TEST SECTION JOINT

TABLE 1

List of Heat Input Section Glass Piping (Top to Bottom)

1. 5.5 inch glass tee piece (inlet)
2. 36 inch long glass pipe
3. 24 inch long glass pipe
4. 12 inch long glass pipe
5. 12 inch long glass pipe
6. 8 inch long glass pipe
7. 8 inch long glass pipe
8. 8 inch long glass pipe
9. 6 inch long glass pipe
10. 6 inch long glass pipe
11. 5.5 inch glass tee piece (outlet)

The end caps used to seal each end of the test section and to align the heating tube are shown in Figure 4. They were constructed from free machining brass plate 0.375 inches thick. Each end plate was bolted to its adjacent glass tee utilizing a teflon gasket ring to provide the glass to brass seal. The seal between the heating tube and the end plate was made with a neoprene 'O'-ring which seated in a sealing groove cut into the brass end plate. The sealing ring is compressed against the end plate and the heating tube by a sealing plate which encircled the heating tube and is bolted to the end plate with three brass machine screws.

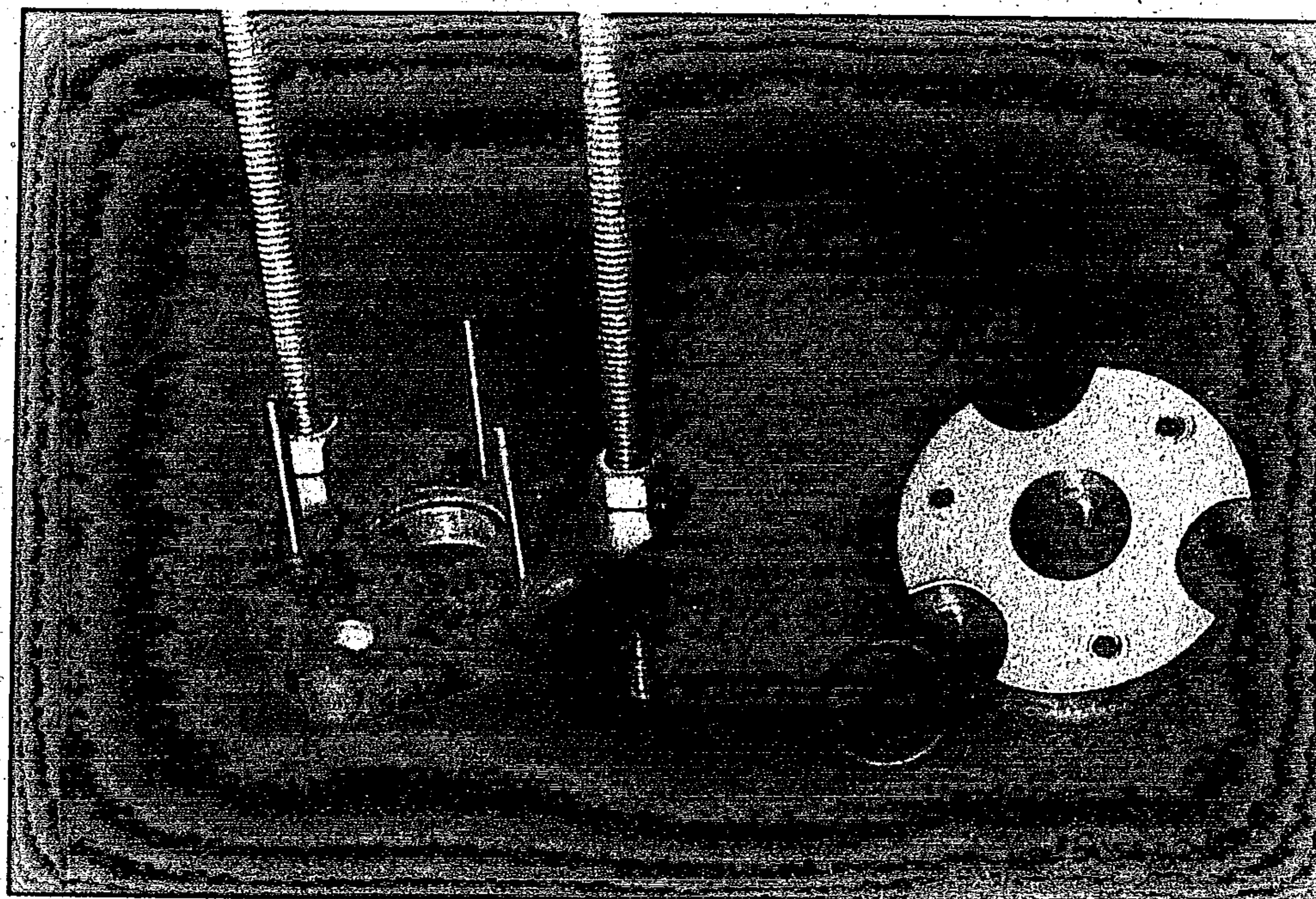

FIG. 4

HEAT INPUT SECTION END SEAL

4. Heaters

Various lengths of heating elements were used singly and in pairs to provide the overall heating lengths tested. These heating elements all have nominal outside diameters of 0.625 inches. To allow these heating elements to slip inside the copper heating tube of the heat input section each heater was ground down on an abrasive wheel such that they would just slip inside the heating tube. The four heaters used consisted of two C1-406R Chromalox "Redhead" Electric Cartridge Heaters with a nominal length of 10.75 inches and rated at 1700 watts in air, one C1-446R Chromalox Cartridge Heater with a nominal length of 36 inches and rated at 3500 watts in air and one C1-458R Chromalox Cartridge Heater with a nominal length of 48 inches and rated at 3800 watts in air. Male and female brass bolt type fittings were machined and brazed on the ends of the heating elements to allow them to be used in paired combinations. Table 2 lists the cartridge heaters and gives the specifications of each heater.

Each heater was powered by a variable autotransformer rated at six kilowatts. The power being dissipated through each heater was obtained by an ammeter-voltmeter circuit which measured the current through the heater and the voltage drop across both heater and ammeter. Each voltmeter has an internal resistance of 5000 ohms/volt and a measuring

TABLE 2
HEATING ELEMENT SPECIFICATIONS

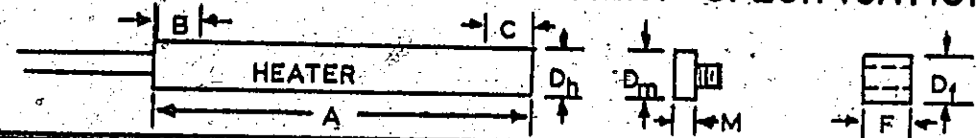

CARTRIDGE ELEMENT	ALL DIMENSIONS IN INCHES							
	HEATER				MALE AND FEMALE END FITTINGS			
	A OVERALL LENGTH	B LEAD END UNHEATED LENGTH	C FITTED END UNHEATED LENGTH	D_h DIAMETER	M MALE D_m LENGTH	M MALE D_m DIAMETER	F FEMALE D_f LENGTH	F FEMALE D_f DIAMETER
C1-406R (M)	10.62	0.50	0.25	.622 ±.002	.067	.600		
C1-406R (F)	10.60	0.67	0.25	as above			.285	.600
C1-446R(M)	35.75	1.00	1.75	as above	.067	.600		
C1-458 R (F)	47.95	1.00	0.75	as above			.375	.600

accuracy of $\pm$ 0.5% full scale with a reading accuracy of $\pm$ .25V, while each ammeter has a measuring accuracy of $\pm$ 1% full scale with a reading accuracy of $\pm$ 0.025 Amperes.

5. Horizontal Connecting Pipe and Riser

In order that the flow area of the connecting tube and riser be approximately equal to the nominal flow area of 0.344 in^2 of the heat input section, 5/8 inch I.D. glass pipe with a flow area of 0.307 in^2 was selected. This selection required the use of a reducing glass section to connect the one inch I.D. outlet of the heat input section to the 24 inch horizontal connecting pipe. The connecting pipe and riser are also Q.V.F. glass pipe to allow visual observations of the single or two phase flow after it leaves the heat input section. The pipe sections are of convenient length to allow temperature and, if necessary, static pressure readings to be made at the joints. Table 3 lists the glass piping used to construct the connecting pipe and riser in order from the reducer section to the top of the riser where it enters the reservoir section. It should be noted that the final 4 inch length of glass pipe is inside the riser such that when the reservoir section is half full, the working fluid just covers the outlet of the riser.

This design was selected since it was felt that it would reduce the flow resistance and improve the chances of operation of the thermosiphon. Further investigation has since revealed that this design choice was not necessary

TABLE 3

List of Connecting and Riser Section Glass Piping

1. 3 inch long one inch to five-eighths inch reducer
2. 24 inch long five-eighths inch glass pipe
3. 2 inch long (each leg) five-eighths inch glass tee piece
4. 36 inch long five-eighths inch glass pipe
5. 8 inch long five-eighths inch glass pipe
6. 6 inch long five-eighths inch glass pipe
7. 6 inch long five-eighths inch glass pipe
8. 10 inch long five-eighths inch glass pipe
9. 12 inch long five-eighths inch glass piping
10. 3 inch long five-eighths inch glass pipe
11. 6 inch long five-eighths inch glass pipe
12. 60 inch long five-eighths inch glass pipe
13. 4 inch long five-eighths inch glass pipe

as there is no noticeable difference if the thermosiphon is operated without the 4 inch pipe in place.

Two types of nylon inserts were used to provide instrumentation access to the flow inside the pipe. One of the nylon inserts as shown in Fig. 5A was used during the first set of tests to determine the effect of an additional pressure drop in the flow loop. As shown in the diagram there were two halves to each insert, one for each side of the orifice plate. Each half of the insert is identical and is constructed in two parts.

One part of the insert is a tapered section machined to fit its individual glass end flare. This part of the insert was drilled out to 5/8 inch I.D. and was machined to have a shoulder which snapped into a retaining groove machined into the second part of the insert. The second portion of the insert is an inch and an eighth O.D. ring with a static pressure tap at the inside edge of the orifice plate side mating surface. All dimensions are as given in Figures 5A and 5B.

The orifice plates used were cut from .007 inch sheet steel. The orifice holes were drilled in this thin stock by clamping each plate between two pieces of 1/4 inch thick perspex and slowly drilling through the sandwiched material. Each plate used had 6 orifice diameters one of which was always 0.625 in. The five other diameters were arbitrarily chosen for each plate from a range of diameter ratios in increments of 0.05 from 0.5 to 0.9; where the diameter ratio

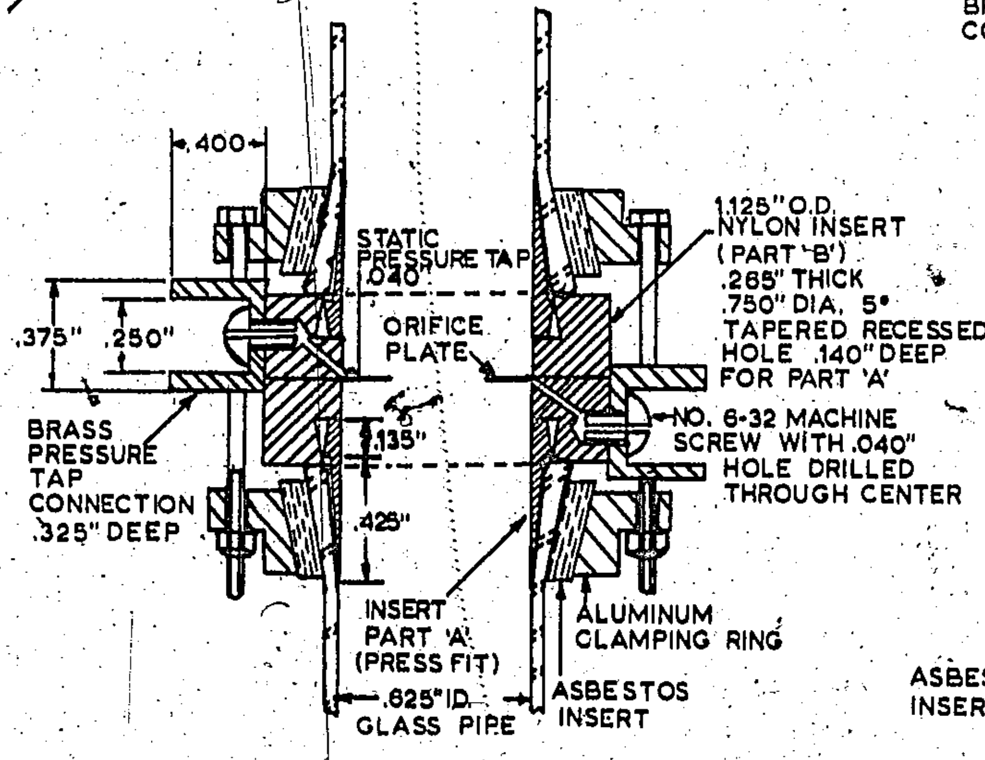

FIGURE 5A

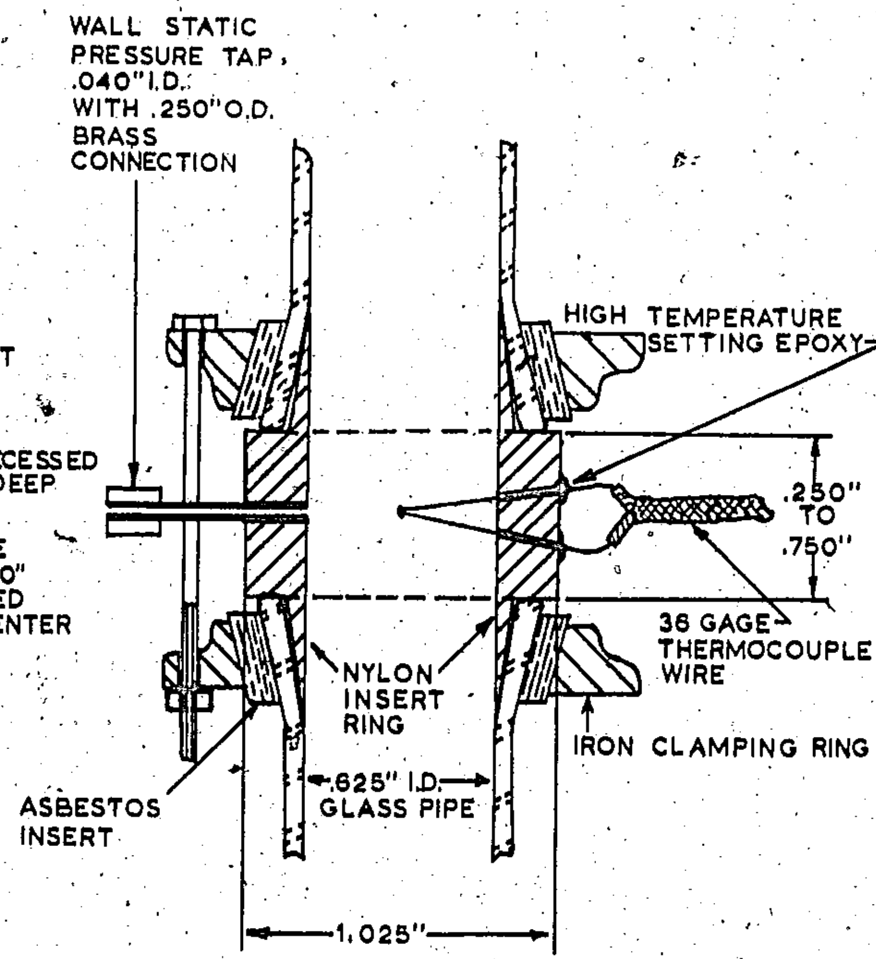

FIGURE 5B

is defined as the ratio of the orifice diameter to adjoining inside pipe diameter.

The number of orifice plates were arbitrarily chosen to be six. The six locations for inserting these plates, as measured from the riser inlet centerline were 2 inches, 46 inches, 67.5 inches, 74 inches, 81 inches, and 92 inches respectively.

The other set of nylon inserts were used whenever the orifice plates were not in use. These inserts, shown in Figure 5B and Figure 5C, were used to allow measurements of centre core fluid temperatures and wall static pressures in the horizontal connecting pipe and riser to be made.

The bottom leg of the riser tee joint contained a nylon insert as shown in Figure 6. This insert was fabricated to reduce the flow losses through the tee and to provide a means of injecting air into the riser to initiate circulation. The insert has a 0.04 inch hole drilled through its longitudinal centre line and it was clamped into the tee piece with an end plate containing an air hose adapter and valve.

6. <u>Thermocouples</u>

Two types of thermocouples were used in the testing program. To measure the bulk fluid temperature at the centre of the annular gap in the heat input section, 0.040 inch O.D. inconel sheathed iron-constantan thermocouples were employed. These thermocouples were calibrated against a copper-constantan

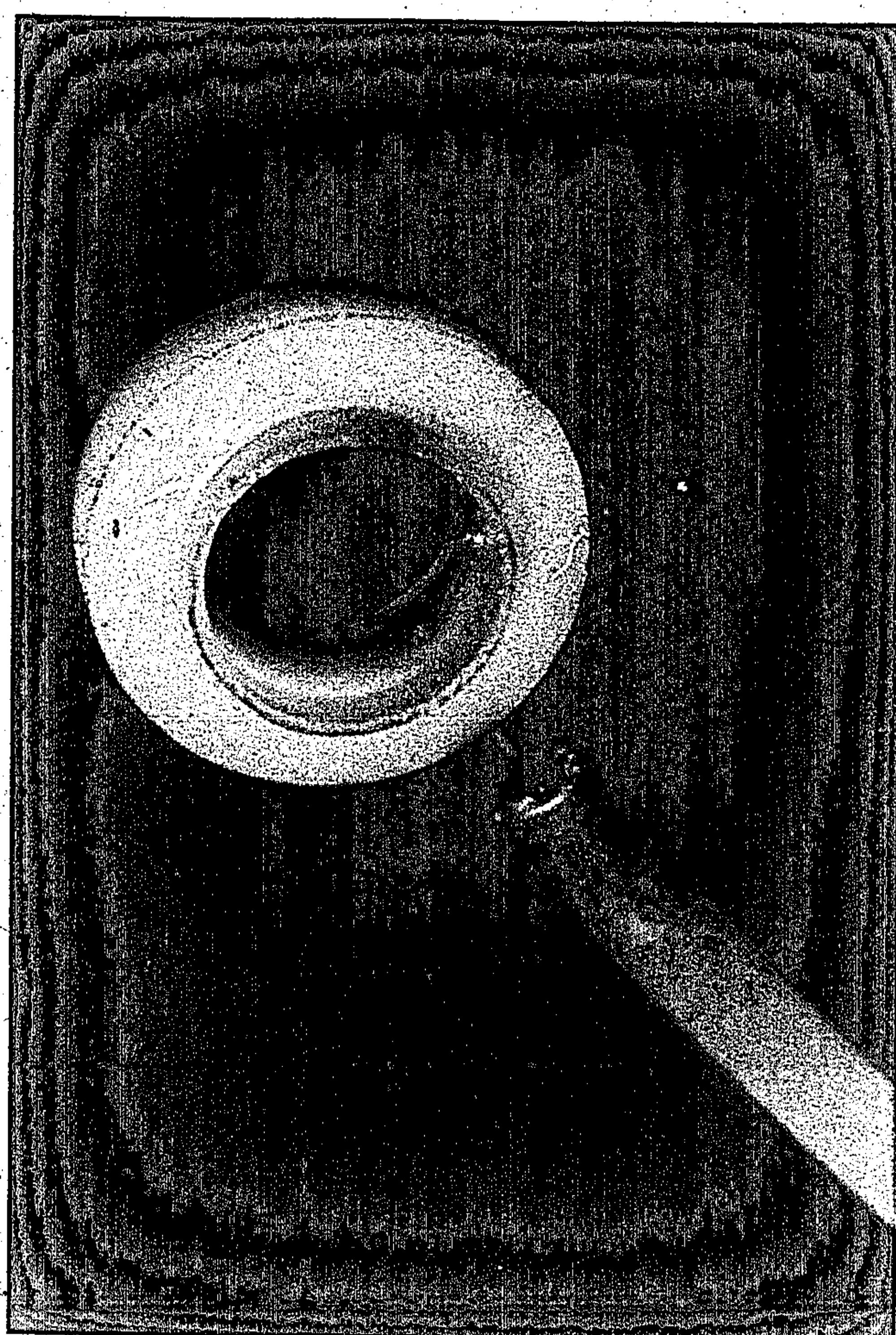

FIG. 5C

NYLON INSERT RING OF RISER

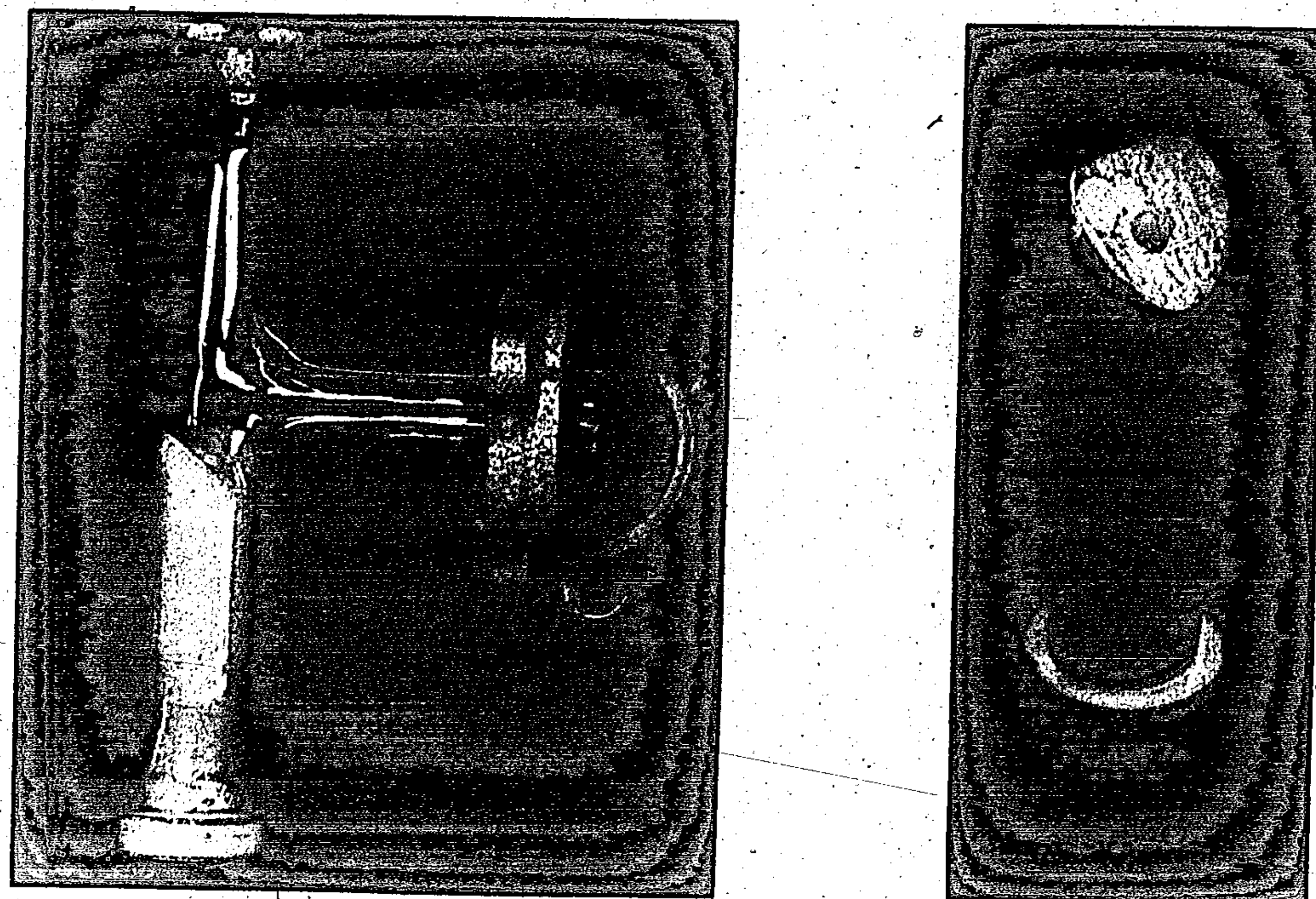

FIG. 6

NYLON INSERT OF RISER INLET "TEE"

thermocouple which was used as the standard reference for all temperature readings. Since the iron-constantan thermocouples were delicate i.e. an estimated head size of 0.010 inches, they were periodically checked for accurate temperature reading by comparing the measured temperature of the circulating working fluid without heat addition against the standard reference thermocouple. Based on the calibration the accuracy of the iron constantan thermocouples is $\pm$ 0.2 F° with a measured reading repeatability of $\pm$ 0.1 F°.

Calibrated copper-constantan thermocouples were used throughout the rest of the thermosiphon loop to monitor temperatures at particular reference points. These 36 gage fiberglass insulated thermocouples were all taken from the same roll and were calibrated against a calibration thermometer in a constant temperature bath according to standard procedures. The accuracy measured for these thermocouples was $\pm$ 0.2 F° with a measured reading repeatability of $\pm$ 0.1 F°. The calibration relationship used to determine the actual temperature from the temperature measured is:

$$T_a = 1.0008\ T_r - 0.0651$$

This relationship was determined by the least squares method of curve fitting and was found to have a correlation coefficient of 1.000.

The temperature readings were taken using two Honeywell millivolt nulling potentiometers each with a limit of error of 0.01 millivolts for a range of 0-16.1 millivolts. Each potentiometer was used for one type of thermocouple wire and was connected to a Thermo-Electric thermocouple switch. Since nulling potentiometers were used and the thermocouples were calibrated through the switch connection it is assumed that there are no reading errors due to any contact resistances between the switch contacts. A Zeref 32°F reference junction unit was used to provide an external reference junction for each circuit and manufactures specifications indicate a maximum reference source error of -0.0, +0.9 F° about 32°F, although the actual errors from measurement are -0.0, +0.1 F°. Temperature conversion calculations were carried out by employing a set of Leed and Northrup Company conversion tables.

7. Venturi

A venturi (see Fig. 7 and Fig. 8) type flow meter was designed to measure the inlet test section flow rate. The venturi design considerations that were considered important were; that the venturi have a very good pressure recovery charact~~eristic and~~, because of the possibility of saturated liquid being present in the reservoir section, that the venturi be located at some point in the thermosiphon loop where the chances of fluid flashing due to the venturi's pressure drop would be minimal.

From a design handbook of flow metering devices used by A.E.C.L. the following design details were chosen:

Diameter Ratio	0.527
Inlet Contraction Angle	7°

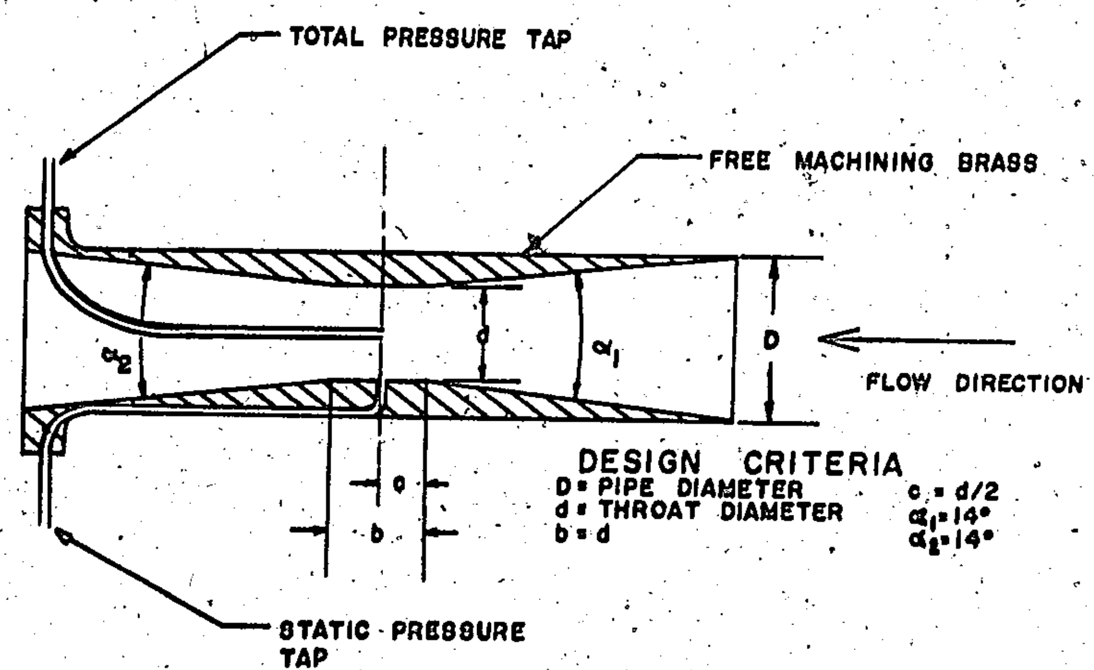

FIG 7
VENTURI DESIGN

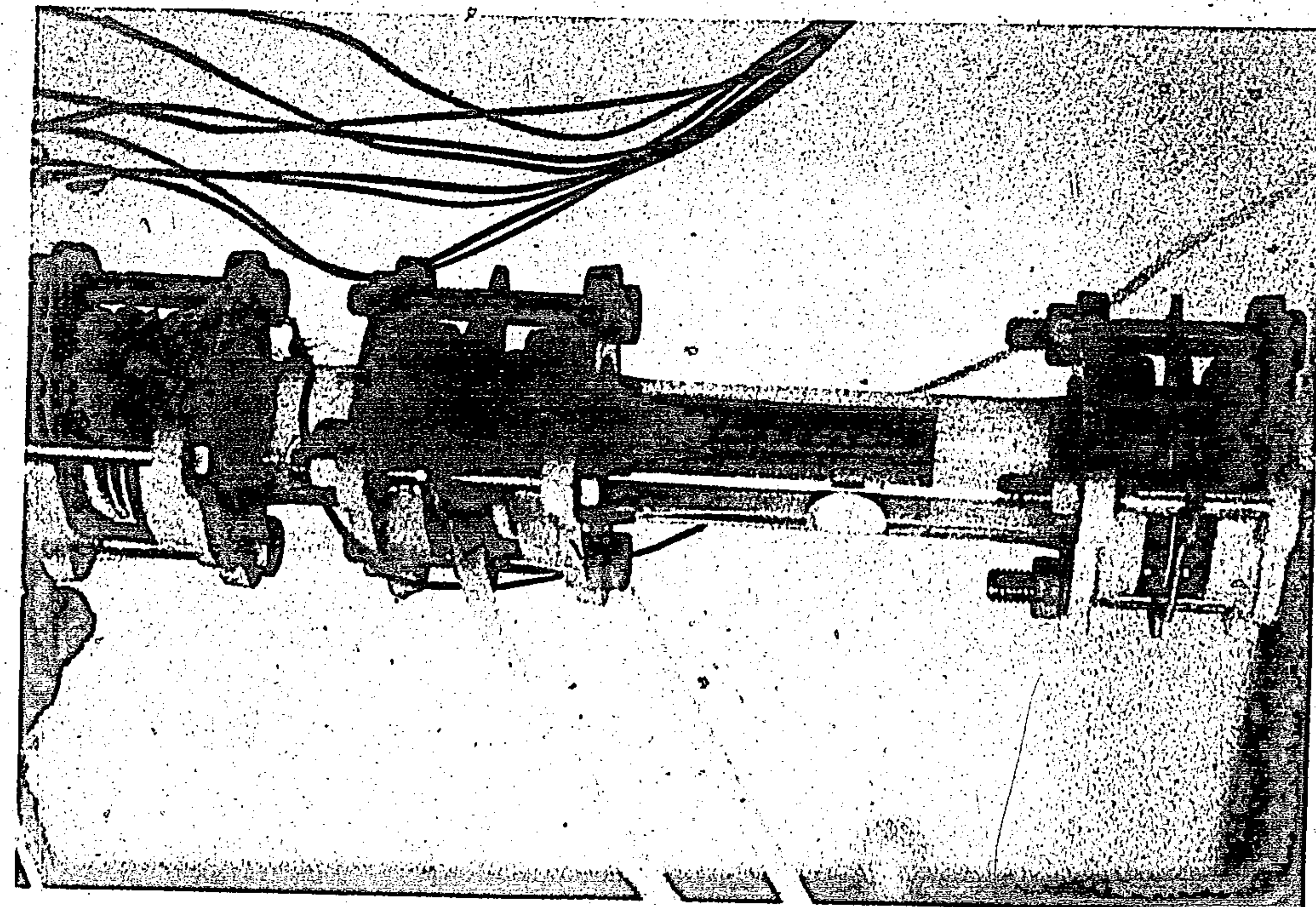

FIG. 8

VENTURI IN PLACE

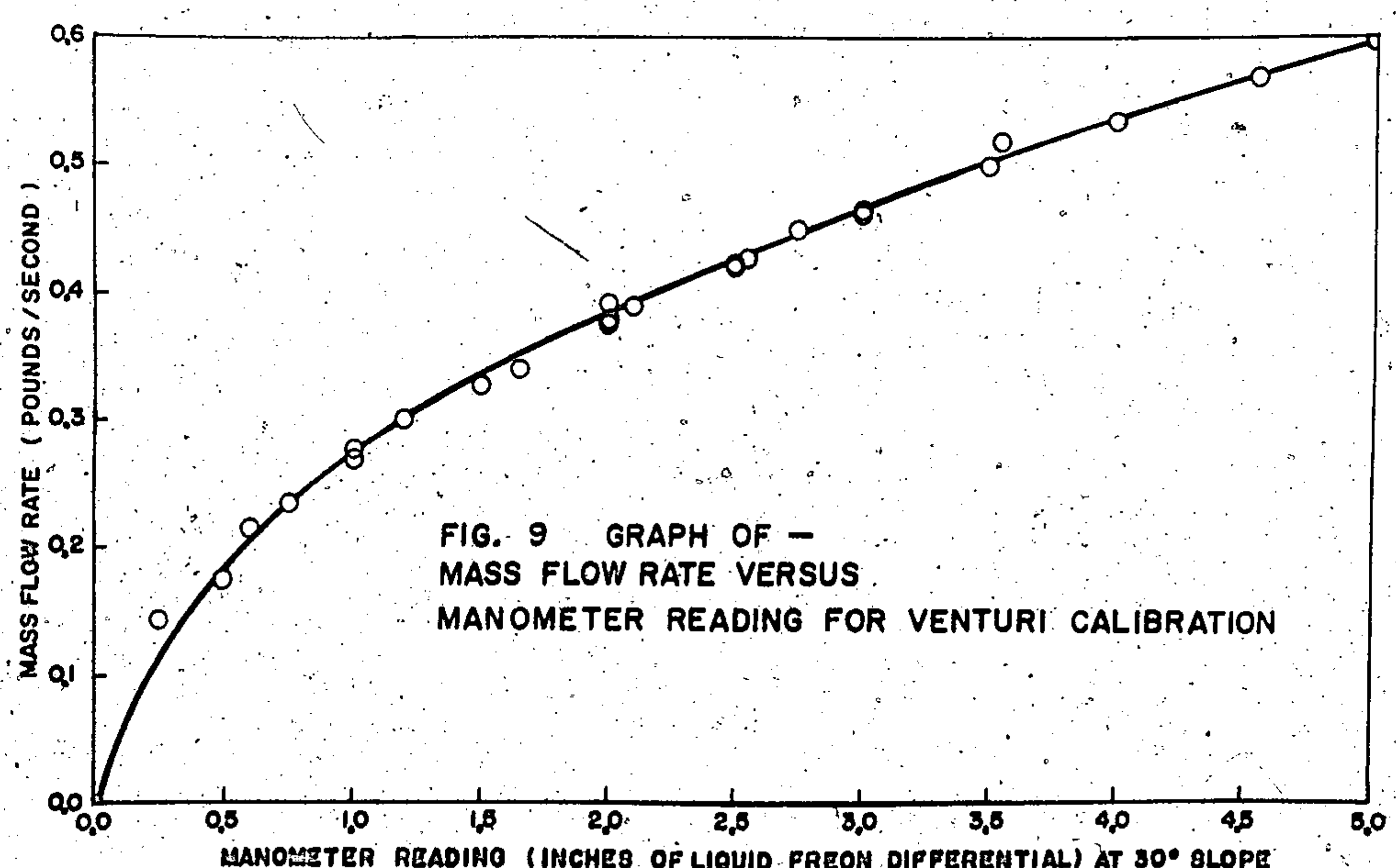

FIG. 9 GRAPH OF —
MASS FLOW RATE VERSUS
MANOMETER READING FOR VENTURI CALIBRATION
MASS FLOW RATE (POUNDS / SECOND)
MANOMETER READING (INCHES OF LIQUID FREON DIFFERENTIAL) AT 30° SLOPE
0,0
0,1
0,2
0,3
0,4
0,5
0,6
0,5
1,0
1,5
2,0
2,5
3,0
3,5
4,0
4,5
5,0

FIGURE 9

Outlet Contraction Angle 7°
Predicted Pressure Loss
in Percentage of Actual
Differential 11%
Location 24 inches below
liquid/vapour interface

The last detail was chosen after assuming that the pressure differential across the venturi would never be greater than 1.3 psi which corresponded to a flow rate of 1.6 pounds per second.

The venturi was calibrated (see Figure 9) in situ using a constant head of Refrigerant 113 as the calibrating liquid. A weighing tank and timer were used to calculate the mass flow rate through the system. The mass flow reading accuracy for calibration was 0.1 lbm with a possible error of .2% with a starting and stopping error estimated as one second for minimum time intervals giving an error of $\pm$ 2% with an overall accuracy of $\pm$ 2.2%. The venturi was installed three inches upstream of the heat input section in a six inch long section of glass pipe. Table 4 lists the glass piping in order from the reservoir cross tee-piece to the heat input section inlet tee-piece.

TABLE 4

List of Inlet Glass Piping

1. 4 inch long 2 inch to 1 inch reducing glass piece
2. 12 inch long glass pipe
3. 3 inch long glass pipe
4. 4 3/4 inch equal 90° bend pipe
5. 6 inch long glass pipe (venturi section)
6. 3 inch long glass pipe

8. Reservoir Section

The reservoir section pipe inside diameter was 2 inches. It is constructed from 4 components: a 2 inch I.D. glass tee piece, each leg being 4 inches long; a 42 inch long section of glass pipe; a 2 inch I.D. glass cross-piece, each leg being 4 inches long and one blank buttress end piece 3 7/8 inches long.

9. Pressure Taps

All pressure taps throughout the system were 0.040 inch I.D. holes drilled into the nylon inserts. After drilling each hole was inspected and any burrs at the edges of the tap holes were removed. Provision for connections to pressure tap lines was made by undersize drilling of the pressure tap outlet such that 0.040 inch I.D. steel hypodermic tubing could be press fitted into the expanded pressure tap hole. The means of connection of the larger bore pressure lines to the hypodermic tubing was a brass reducer ferrule silver soldered to the free end of the hypodermic tubing. The ferrule size was such that the connecting tubing of the pressure lines slip tightly over the ferrule.

The only exception to the above were the fittings on the nylon inserts for the orifice plates. In this case a hollow no. 6-32 screw was used to connect a 1/4 inch O.D. brass connecting piece to the nylon insert as shown in Figure 5A.

10. Manometers

Two types of manometers were used for measuring pressures in the system. One type was a mercury-in-glass U-tube manometer open to the atmosphere used to indicate static pressures. The tubing used was 0.075 inch I.D., 0.187 inch O.D., 30 inch long standard manometer glass tubing mounted vertically in front of 1/20th inch per division graph paper and a reading accuracy of 0.05 inches. The connection between the system and manometer was 0.185 inch I.D. flexible hard polyvinyl tubing. Measurements were made of the damping of the system as calculated from experimental data and it was found that the damping factor was 0.59 at a natural frequency of 0.6 Hz with the system fully charged with the working fluid.

To indicate differential pressures, inverted, 22 inch long, sloping U-tube glass manometers were used. Each manometer was constructed from 0.060 inch I.D., 0.250 inch O.D. precision bore glass tubing with a branch at the top of the U to provide a port for injection or withdrawal of the manometer working fluid. Sealing of the bleed branch was by means of a standard automotive, brass tire valve connected to the manometer by a short length of neoprene tubing. The connecting lines from the manometer tubes to the 0.040 inch I.D. hypodermic tubing pressure taps were 0.185 inch I.D. flexible hard polyvinyl tubing connected to the manometer by short lengths of neoprene tubing.

Some problems were encountered with the design of the sloping tube manometers. The differential pressure manometers used for measuring pressure losses between pipe joints, differential pressure across orifice plates and venturi differential pressure were originally designed for using mercury as the measuring fluid. From preliminary testing it was found that mercury was not satisfactory for several reasons; these being that the manometers would require only a 2 1/2 to 3 degree tilt from horizontal, introducing a large possible reading error and that because of the low surface tension of R-113 the mercury would trap globules of the refrigerant against the manometer tube wall resulting in changes in actual cross-sectional tube area.

A fluid that was immiscible in R-113 and that would allow a slope sufficiently large so as to reduce the probable reading errors was diligently sought for without a satisfactory solution. Water was ruled out because of similar surface tension problems as the mercury-R113 situation. Other standard manometer fluids were also tried but they had other drawbacks such as the fluid colouring being bleached out or absorbed by the working fluid so that it was impossible to locate the interface between the two liquids.

Finally it was decided to use an inverted manometer with a 30° slope using air as the displacing medium although this meant putting up with time consuming checks for leaks and extra care taken in purging the tubes and lines of extraneous air bubbles. This decision cleared all problems of differential pressure measurement except for large overall system pressure drops and these were simply solved by using similar manometer tubes with an overall length of 30 inches mounted vertically. The measurement scale for all of these manometers was 1/10 inch per division graph paper with a reading accuracy of 0.1 inches.

C. <u>Experimental Procedure to Run a Test</u>

The procedure for a testing sequence is:

1. a previous determination of the type of testing to be conducted will dictate whether:

   a. An orifice plate of a particular diameter ratio is inserted in the riser section at some elevation above the bottom glass tee-piece inlet centerline or:

   b. A chosen combination of heating elements is inserted in the heating tube of the heat input section and located at a particular position relative to the outlet centerline of the heat input section.

2. Turn on the thermocouple reference junction.

3. Make all necessary connections to the power supplies being used.

4. Charge the system with the working fluid by pressurising its storage container and forcing the working fluid into the system through a valve located at the bottom of the heat input section.

5. Check for any leaks in the thermosiphon loop as the working fluid slowly rises to the fill line.

6. Purge any trapped air from the manometer lines by squeezing the neoprene connecting tubes at the bottom of the manometers.

7. Check level of working fluid in reservoir section and top off to desired fill line.

8. Check for zero reading on manometers.

9. Initiate circulation by injecting air at the bottom of the riser section.

10. Switch on thermocouple potentiometers and check settings of reference junction and standard cell compensation circuits.

11. Compare temperature readings of the thermocouples in the system.

12. Record barometric pressure.

13. Supply sufficient power to heating element(s) to provide a uniform heat flux capable of sustaining circulation after air injection in the riser section ceases.
14. Decrease rate of air injection gradually as the temperature of the working fluid increases and boiling commences in the riser.
15. Stop air injection and allow the system to stabilize.
16. Vary heat flux slowly to achieve either minimum heat input test or maximum heat input test.
17. Allow system parameters to reach steady state before taking readings.
18. After system start up, changes in heating element position were carried out at reduced power input while the system is operating. If the change in heater location is done slowly the system will have sufficient time to adjust to the change but if the change is too rapid it will usually cause a reversal.
19. During a flow reversal the heating element(s) were powered down. This was done since it was found that several changes in flow direction would usually take place and it is often quite possible to reacquire the desired flow direction by repowering the heating element(s) at the proper moment.

If this is not done it is necessary to return to step 9, jump to step 14 and continue from that point to run another test.

20. For orifice plate testing it is necessary to drain the system and start at step 1, jump to step 5 and run through the rest of the test sequence omitting steps 10, 11 and 12.

21. Because of Refrigerant 113's ability to dissolve oils it was necessary to periodically change the working fluid used in the system. The contaminated fluid was run through a distillation apparatus to remove the contaminants and then re-used in the system.

IV RESULTS

1. Introduction

All the information gathered from the tests conducted with the thermosiphon loop have been collected and collated for presentation in this chapter. The information presented covers the Preliminary Operating Tests, the Orifice Plate Experiments, the Heater Experiments and a presentation of notable photographically recorded observations.

1.1 Preliminary Operating Tests

When construction of the system was completed the initial attempts to achieve sustained downflow operation using the 22 inch heating unit were unsuccessful. Visual observation of the flow indicated that as the rate of air injection at the bottom of the riser was decreased, to enable the bouyancy forces created by the flashing liquid to take over, the flash point in the riser would start to vary periodically with time. This fluctuation caused periodic changes in flow rate and in the amount of vapour on the heating surface. These fluctuations increased in amplitude ultimately causing a reversal of flow.

Because of the large amount of vapour being generated on the 22 inch heating surface it was decided that longer heaters with a reduced heat flux would likely be more successful. In addition, it was decided to insert a flow restriction in the riser to act as a flash initiator by causing an abrupt drop in the fluid pressure across the device. The use of a flow restriction in the form of an orifice plate in fact made sustained reversed flow possible with the 22 inch heating unit.

This success lead to an investigation of the operating limits imposed on the heat input to the system when the size and location of the orifice plate was varied in the riser. The use of longer heaters in the heat input section was also found to improve the operating range of the system and lead to an investigation of the effect of various heater lengths and positions on the system performance.

The results of these investigations are presented in the following sections along with the pertinent photographic or visual observations.

Although the raw and subsequent reduced data has not been included in this thesis, it has been collected in a single volume and is available in the Mechanical Engineering Office Library as Report HT-73-I entitled "Data Summary of the Reversed Flow, Boiling Thermosiphon Loop Tests for Master's Thesis" by R. Gaspar. Sample data however has been included in Appendix II.

1.2 Orifice Plate Experiments

Experiments to determine the effect of various sizes and locations of orifices were conducted in the riser. The orifices tested had a range of (orifice diameter/riser diameter) ratios from 0.5 to 1.0 in increments of 0.05 and could be positioned 2 inches, 46 inches, 67.5 inches, 74 inches, 81 inches or 92 inches above the inlet "Tee" centerline.

The effect of the orifice plate diameter ratio on the heat input limits is shown in Figure 10 which indicates that there is little variation in the maximum heat input until the diameter ratio drops below approximately 0.6. It also indicates that there is little variation in the minimum power input with the exception of a diameter ratio of 1.0, at which point the minimum heat input required to maintain reversed flow is significantly higher. This demonstrates that an orifice plate can be used to further lower the minimum power requirements of a reversed flow system if the situation requires such a reduction. It should be pointed out that such a system operating with an orifice plate in the riser and with minimum heat flux is susceptable to premature reversal if the change in heat input is too large.

The reason for this instability is readily apparent from an inspection of Figure 10 which shows two operating modes, the smaller of these being a range of minimum heat flux where flow oscillations occur but do not lead to reversal. This range of oscillating reversed flow does not exist for diameter ratios approaching unity. Also to be noted is that the changeover point from stable reversed flow to oscillating reversed flow is not a function of diameter ratio except when no orifice is present.

The stable operating range indicated in Figure 10 is much larger, the flow rate is steady and the system is

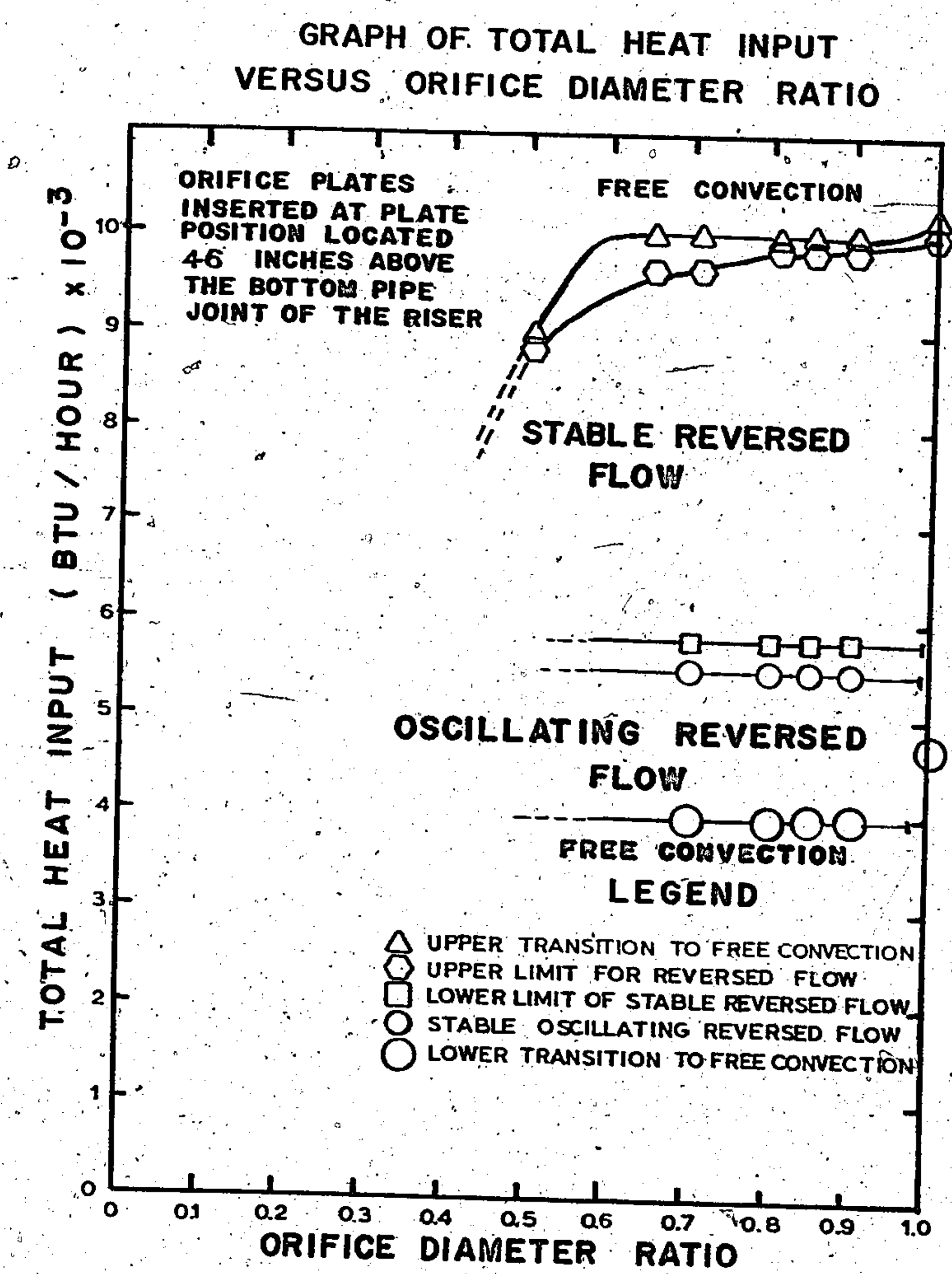
GRAPH OF TOTAL HEAT INPUT
VERSUS ORIFICE DIAMETER RATIO
ORIFICE PLATES INSERTED AT PLATE POSITION LOCATED 46 INCHES ABOVE THE BOTTOM PIPE JOINT OF THE RISER
FREE CONVECTION
STABLE REVERSED FLOW
OSCILLATING REVERSED FLOW
FREE CONVECTION
LEGEND
UPPER TRANSITION TO FREE CONVECTION
UPPER LIMIT FOR REVERSED FLOW
LOWER LIMIT OF STABLE REVERSED FLOW
STABLE OSCILLATING REVERSED FLOW
LOWER TRANSITION TO FREE CONVECTION
TOTAL HEAT INPUT (BTU / HOUR) x 10⁻³
0
1
2
3
4
5
6
7
8
9
10
0
0.1
0.2
0.3
0.4
0.5
0.6
0.7
0.8
0.9
1.0
ORIFICE DIAMETER RATIO

FIGURE 10

not as sensitive to sudden or large changes in heat flux.

Figure 11 indicates that there is no significant variation in maximum heat input when an orifice plate with a fixed diameter ratio is used and its position in the riser is changed.

The following visual observations of the thermosiphon loop were noted:

1. The presence of an orifice plate at any location in the riser caused a periodic fluctuation in flow rate evidenced by a change in flash point position for heat input values near either the maximum or minimum values required to maintain reversed flow.
2. Flow separation from the riser wall was noted to occur on the downstream side of the orifice plate for diameter ratios of 0.7 or less at locations 45 inches or higher above the riser inlet centerline and did not necessarily indicate the starting point for flashing. Also the flow separation disappeared or diminished in extent when flashing commenced upstream of the orifice plate.
3. Perturbations of the order of 300 Btu/hour of either increase or decrease in heat input could initiate cyclical changes in the location of the flashing point in the riser when the system was operating in the stable operating range. These

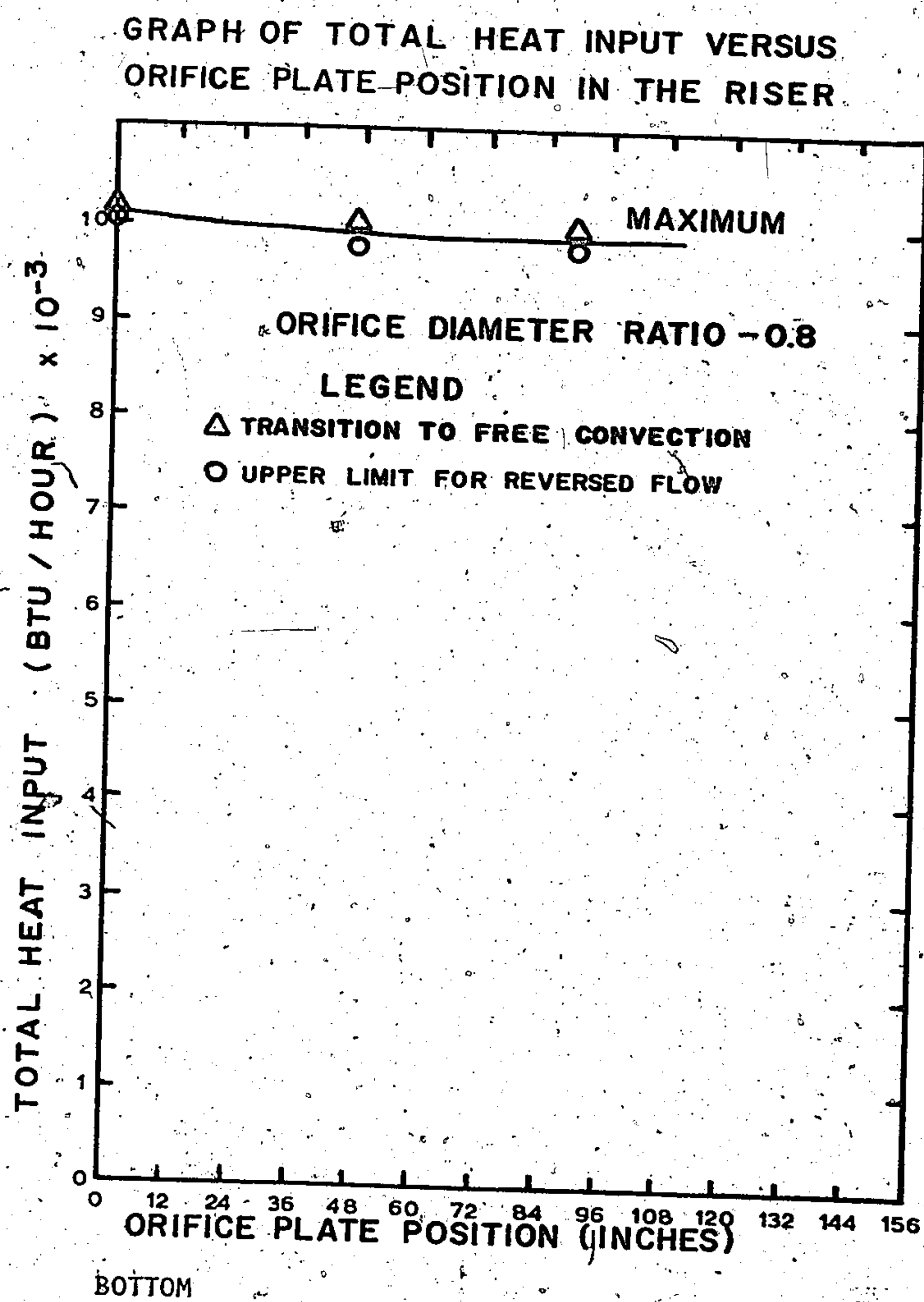
GRAPH OF TOTAL HEAT INPUT VERSUS
ORIFICE PLATE POSITION IN THE RISER
MAXIMUM
ORIFICE DIAMETER RATIO - 0.8
LEGEND
△ TRANSITION TO FREE CONVECTION
○ UPPER LIMIT FOR REVERSED FLOW
TOTAL HEAT INPUT (BTU / HOUR) x 10-3
0
1
2
3
4
5
6
7
8
9
10
0
12
24
36
48
60
72
84
96
108
120
132
144
156
ORIFICE PLATE POSITION (INCHES)
BOTTOM
TOP

FIGURE 11

cyclical changes affected both the flow rate and the heater section outlet temperature such that the system would continue to hunt for a stable flash point location. Generally the system was capable of attenuating the oscillations allowing a stable flash point to be reached. However if the heat input was near the maximum, reversal in flow direction would accompany the oscillations.

4. After a number of shorter lengths of piping were used to construct the riser to allow for insertion of orifice plates and instrumentation it became evident that, with no vapour carryover, the piping joints were producing nucleation sites for flashing even when the orifice plates were not used. With vapour carryover from the heat input section the location of the flash point was seen to be independent of the pipe joints. The bubbles of vapour appeared to provide all the necessary nucleation sites in the riser.

6. The length of time required for the system to reach steady state was sometimes as long as 15 minutes for step changes in heat input of 150 Btu/hour when the system was operating near the maximum heat input value. In fact on several occasions with orifice plates in place flow reversals took

place after steady state had apparently been reached and data was being recorded.

7. Static electricity charges were noted to exist on the outer surface of the glass riser.

1.3 <u>Heater Length-Position Experiments</u>.

Tests were conducted to determine the effect of varying the length and position of the heat input units on the operating characteristics of the thermosiphon loop. The experiments conducted were carried out for the following range of variables:

Heating Lengths. 11, 22, 36, 48, 60 and 84 inches

Position of the Lower End of Heater Relative to Heater Section Outlet Centerline. 0 to 50 inches

For the variables listed it was determined that overall these tests the rate of heat input varied from a minimum of 3,500 Btu/hour to a maximum of 12,000 Btu/hour. The corresponding flow rates measured varied from a minimum of 0.383 lb/sec to a maximum of 0.485 lb/sec.

Before going further it should be noted that all graphs which refer to the heaters are based on the true heated length of each unit, not on the nominal physical length by which they are designated in this thesis.

1.3.1 System Output Quality.

In order to compare the overall evaporation performance of the various configurations tested a term Output Quality "X" was defined as follows:

X = Heat added per pound to raise the enthalpy above the saturation enthalpy at the condenser pressure/Heat required to completely vaporize one pound of fluid at the condenser pressure. Symbolically this expression may be written as

$$X = \frac{h_{out} - h_{sat}}{h_{fg}} \qquad \text{Eqn. 7}$$

or, to more clearly indicate its origin, as:

$$X = \frac{(h_{out} - h_{in}) - (h_{sat} - h_{in})}{h_{fg}} \qquad \text{Eqn. 8}$$

where the first term in the numerator of Equation 8 is the enthalpy rise in the heat input section and the second term is the enthalpy rise necessary to bring the fluid at inlet up to the saturation enthalpy in the condenser.

To further simplify the calculation of the quality, Equation 7 can be rewritten in terms of temperatures. This method of calculation was selected rather than finding a correlating equation for h_{out} versus T_{out} because the numerator of Equation 7 can be replaced by $C_p(T_{out} - T_{sat})$ since the specific heat at constant pressure is commonly given in a table of properties of most liquids. Thus we have

$$X = C_p \frac{(T_{out} - T_{sat})}{h_{fg}} \qquad \text{Eqn. 9}$$

As the calculations which were carried out for this thesis were in the form of a program for a Hewlett Packard 9100B calculator, an expression for h_{fg} in terms of T_{sat} was determined. This was done to allow the operator to input only two variables, T_{out} and T_{sat}. Thus the efficiency calculation is based on two measurements; the condenser operating pressure which can be converted to a corresponding saturation temperature and the heat input section outlet temperature. Thus the final equation used for computational purposes with appropriate numerical values is:

$$X = \frac{0.277\ (T_{out} - T_{sat})}{72.179 - 0.077\ T_{sat}} \qquad \text{Eqn. 10}$$

1.3.2. Comparison of Heater Performance

Figure 12, a graph of system output quality versus length of heating element for the lower end of the heating element located at the outlet centerline of the heat input section, indicates the minimum and maximum qualities achieved by the thermosiphon.

Note that the minimum operating quality is not a function of the heater length except for a lower limit on the length of a heater which would be capable of sustained operation. This limit is indicated by the intersection of the extrapolated curves. The curve for the upper limit output quality increases assymptotically with the length of the heater.

The effects on the output quality caused by changing

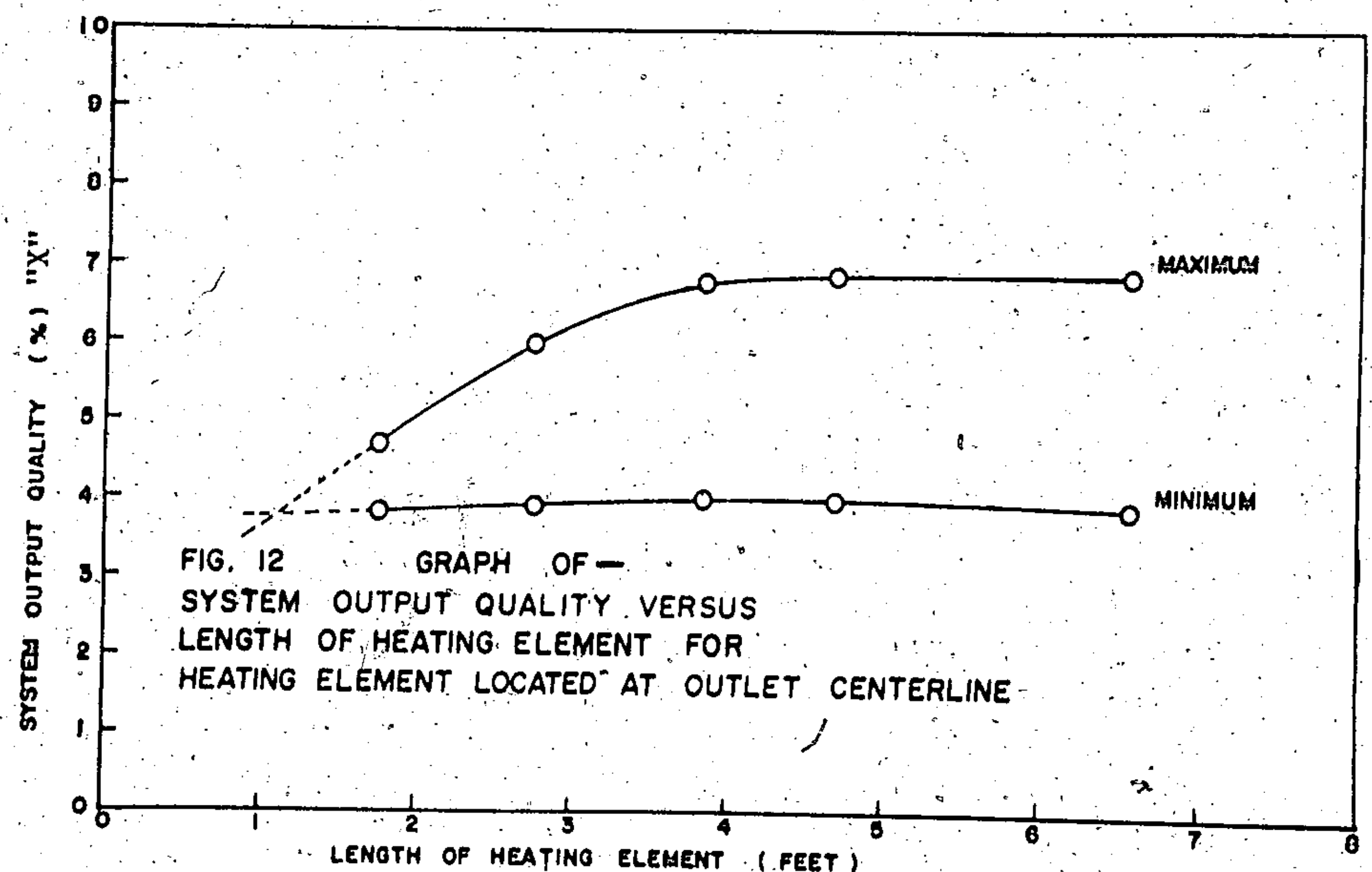
FIG. 12 GRAPH OF —
SYSTEM OUTPUT QUALITY VERSUS
LENGTH OF HEATING ELEMENT FOR
HEATING ELEMENT LOCATED AT OUTLET CENTERLINE
MAXIMUM
MINIMUM
SYSTEM OUTPUT QUALITY (%) "X"
LENGTH OF HEATING ELEMENT (FEET)
0
1
2
3
4
5
6
7
8
9
10

FIGURE 12

the vertical position of the heating elements in the heat input section are illustrated in Figure 13. This graph of system output quality versus position of the bottom end of the heating element above the outlet centerline compares the output qualities achieved by the five heaters listed. The graph shows that in addition to the previously noted fact that the minimum output quality is not a function of heater length, the minimum is also not a function of heater position. The graph also indicates that there is a decrease in output quality as the heater is elevated above the outlet centerline, the longer heaters being more adversely affected.

A situation which is also evident is the intersection of efficiency values for the 36 inch heater with the values for the 48 inch and 60 inch heaters. In order to resolve this apparent discrepancy further testing of the 36 and 48 inch heaters was undertaken. Unfortunately a modification had already been made to the heat input section in the form of an instrumented heated surface as described in Chapter III, section 3. Figure 14, a graph of system output quality versus heating element position above outlet centerline illustrates the results of this additional testing. As can be seen in the graph the output qualities of the two heaters appear to converge but do not intersect.

It was observed that the output qualities of the 36 inch and 48 inch heaters are slightly lower than those for similar positions in Figure 13. In addition the slope

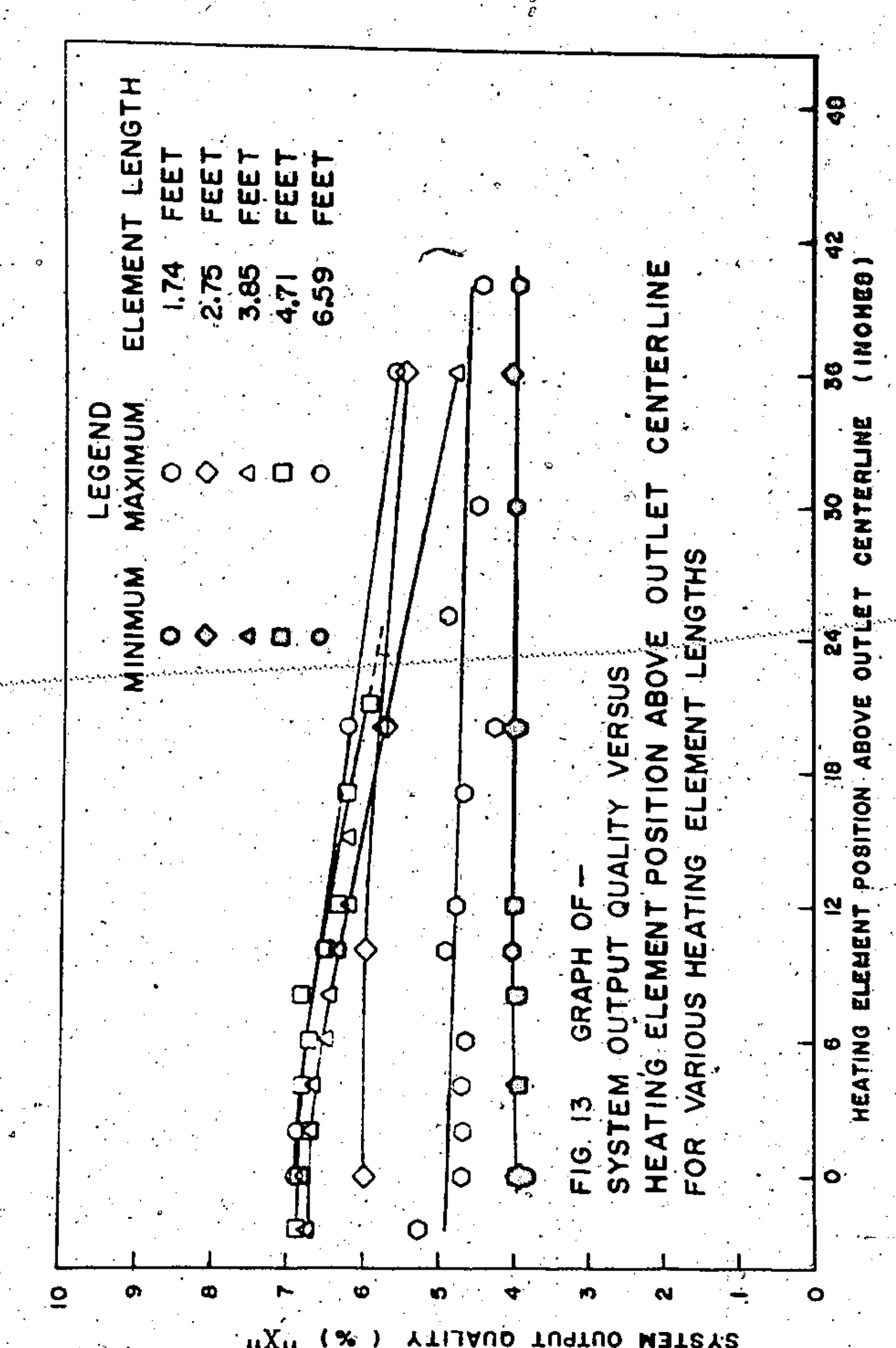
LEGEND
MINIMUM MAXIMUM ELEMENT LENGTH
1.74 FEET
2.75 FEET
3.85 FEET
4.71 FEET
6.59 FEET
FIG. 13 GRAPH OF —
SYSTEM OUTPUT QUALITY VERSUS
HEATING ELEMENT POSITION ABOVE OUTLET CENTERLINE
FOR VARIOUS HEATING ELEMENT LENGTHS
HEATING ELEMENT POSITION ABOVE OUTLET CENTERLINE (INCHES)
0
6
12
18
24
30
36
42
48
SYSTEM OUTPUT QUALITY (%) "X"
0
1
2
3
4
5
6
7
8
9
10

FIGURE 13

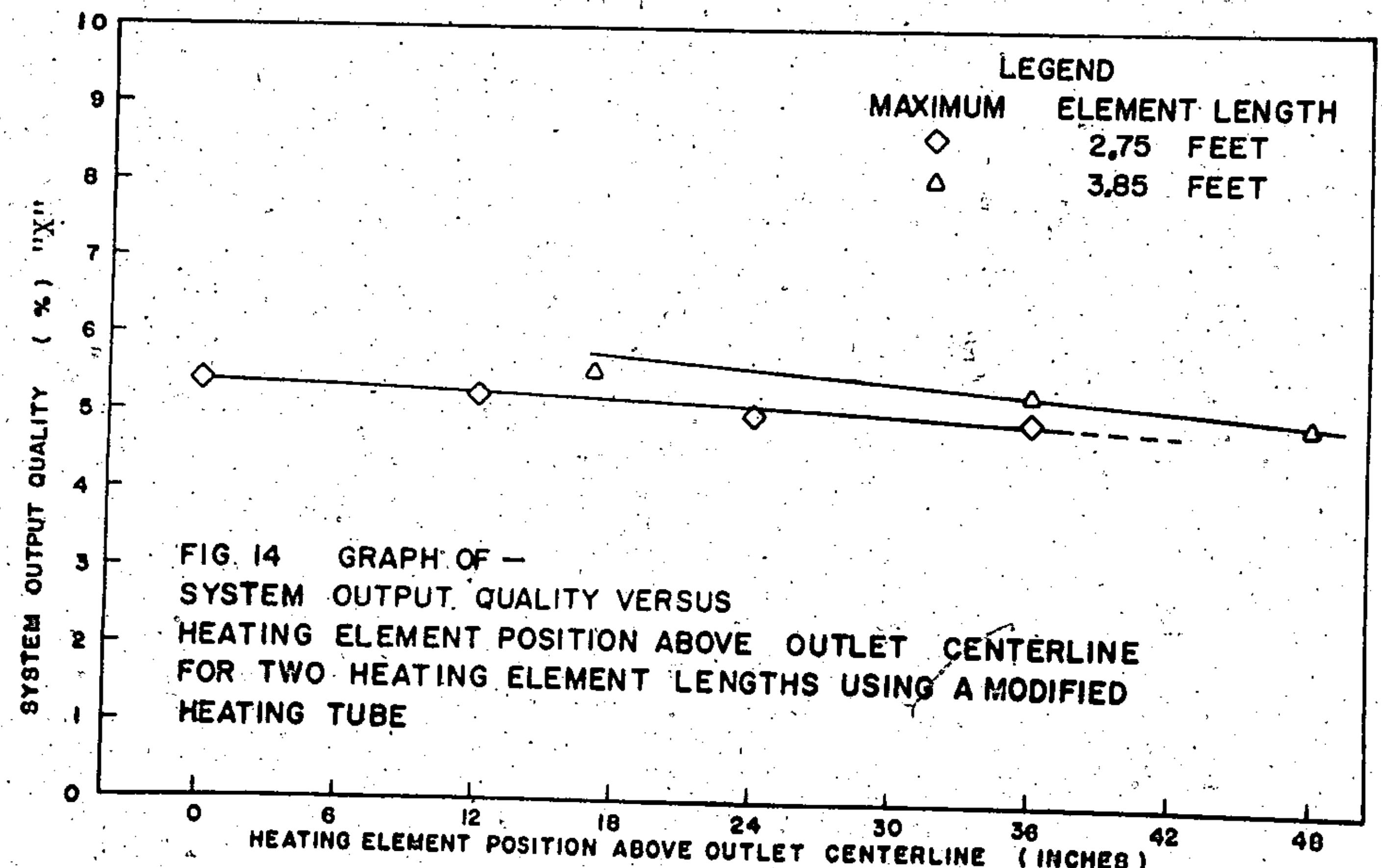
LEGEND
MAXIMUM ELEMENT LENGTH
◇ 2.75 FEET
△ 3.85 FEET
FIG. 14 GRAPH OF —
SYSTEM OUTPUT QUALITY VERSUS
HEATING ELEMENT POSITION ABOVE OUTLET CENTERLINE
FOR TWO HEATING ELEMENT LENGTHS USING A MODIFIED
HEATING TUBE
SYSTEM OUTPUT QUALITY (%) "X"
HEATING ELEMENT POSITION ABOVE OUTLET CENTERLINE (INCHES)
0
1
2
3
4
5
6
7
8
9
10
0
6
12
18
24
30
36
42
48

FIGURE 14

of the output quality curve for the 36 inch heater in each of the graphs was practically identical. It was felt that the 12.7% displacement of the output quality curve for the 36 inch heater was due to the replacement of approximately 18% of the copper heating surface with epoxy filler over the thermocouple leads. This increases the copper surface heat flux for a given power input since epoxy conducts heat to a lesser degree than copper. Thus the author believes that the multiplication of the values of Figure 14 by 1.127 to bring the two 36 inch long heater test results into line was warranted.

To arrive at a corrected graph of system efficiency versus heating element position, one final correction was made for all heaters and this was to take into account the unheated bottom end of each heater. This unheated portion is due to insulating end seals and allowances for internal connection of the lead wires. Thus Figure 15, a graph of system output quality versus corrected heating element position above outlet centerline, is the final outcome of combining the information of Figures 13 and 14 and also indicates a correct placement of the bottom end of each heater accurate to $\pm$ 1/8 inch.

The graph shows that the trends in output quality are the same for the 48 inch, 60 inch and 84 inch heaters although each successively longer heater improves the output quality very slightly. What can also be noted is that the

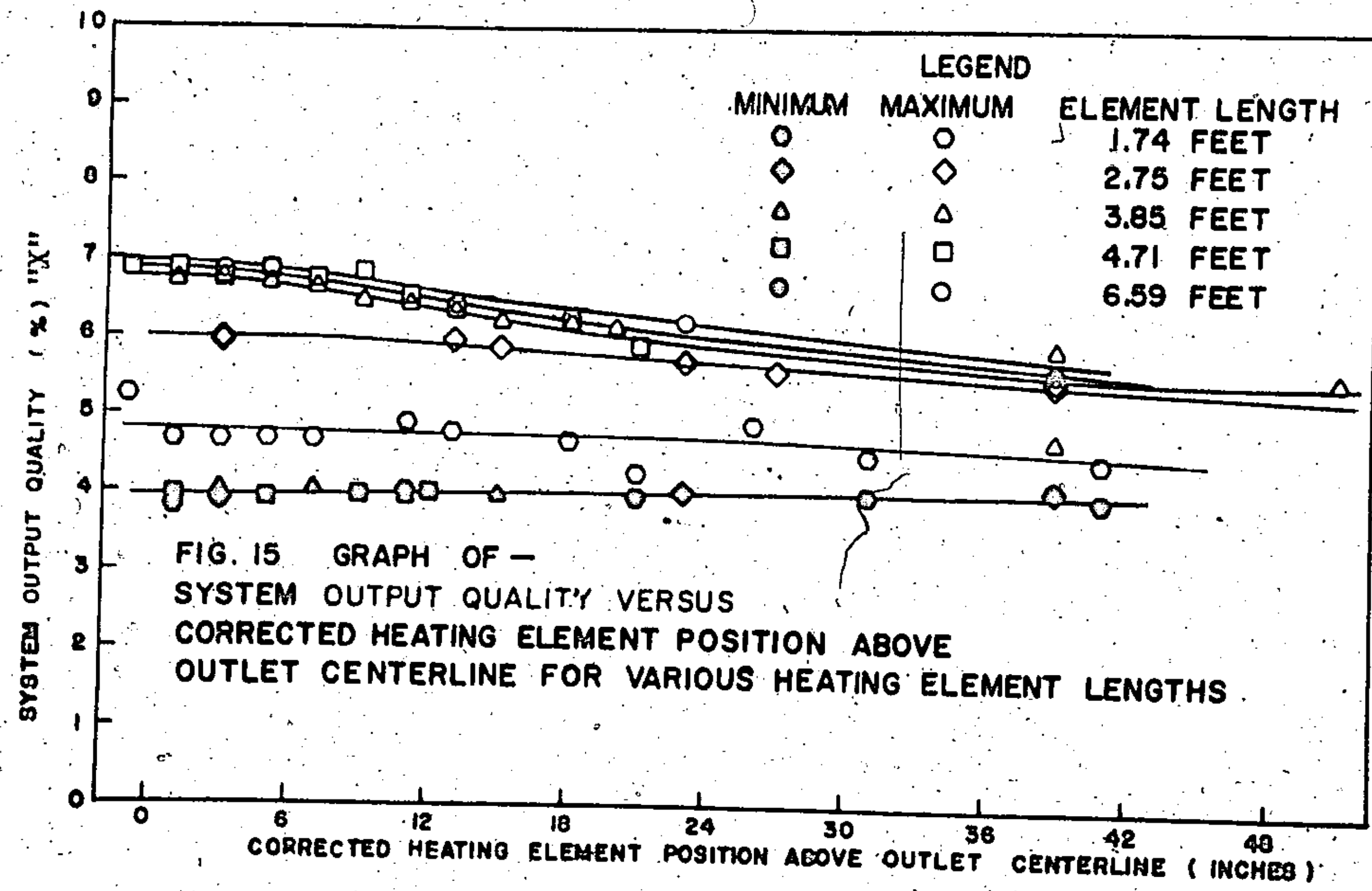

FIG. 15 GRAPH OF —
SYSTEM OUTPUT QUALITY VERSUS
CORRECTED HEATING ELEMENT POSITION ABOVE
OUTLET CENTERLINE FOR VARIOUS HEATING ELEMENT LENGTHS

FIGURE 15

36 inch heater has an output quality line which approaches the operating curves of the three previously mentioned heaters at the 40 inch position and appears to then run parallel to them. The rest of the graph shows the same information previously discussed for the minimum output quality line of the system.

One piece of additional information relating to the 22 inch heater should be discussed and this concerns the scatter of data points in both Figures 13 and 15. The scatter was caused by minor flow instabilities in the heating section and the only time these appeared was during the testing of the 22 inch heater. These instabilities were characterized by a cyclical change in the amount of vapour being generated on the heating surface and these changes were observed to diminish as the heat flux increased or the heater was moved higher in the heat input section.

For low elevations of the heater the cyclical changes disappeared when the heat input reached such a level that areas of the heating surface were no longer in contact with the coolant flow. Indeed, the ability of the system to operate with dry patches on the heating surface, as shown in Figure 20, was another characteristic of this heater length which was not observed during testing of the rest of the heaters. Since it was felt that the system should not operate with dryout the maximum output quality of the 22 inch heater was determined by the value at which dryout appeared and because this limit is determined by observation of dry patches rather than a flow reversal there is significantly more scatter in this data.

1.3.3. Additional Information and Photographic Observations

Figure 16, a graph of mass flux versus heating element length for the bottom end of the heating element located at outlet centerline, indicates the small variation in mass flux exhibited by the system as the heat input was increased from the minimum to the maximum value required for stable operation.

Figure 17 is an enlarged photo of the outlet tee of the heat input section and illustrates the bubble distribution as well as showing the relatively large voids which may become attached to the heat input section outer wall. This condition generally indicates that a flow reversal is imminent.

Figure 18 is a photo of the outlet tee taken when the system was near reversal. This picture shows a different characteristic of the system which can be used to help predict when the maximum heat input has been reached. This characteristic is the formation of a large, irregular bubble in the side branch of the heat input section outlet tee. This bubble may grow in size until it occupies one-half of the outlet flow area before a reversal occurs.

Figure 19 is a view of part of the heat input and horizontal sections. The picture shows the void being produced on the heating surface as well as the helical vapour

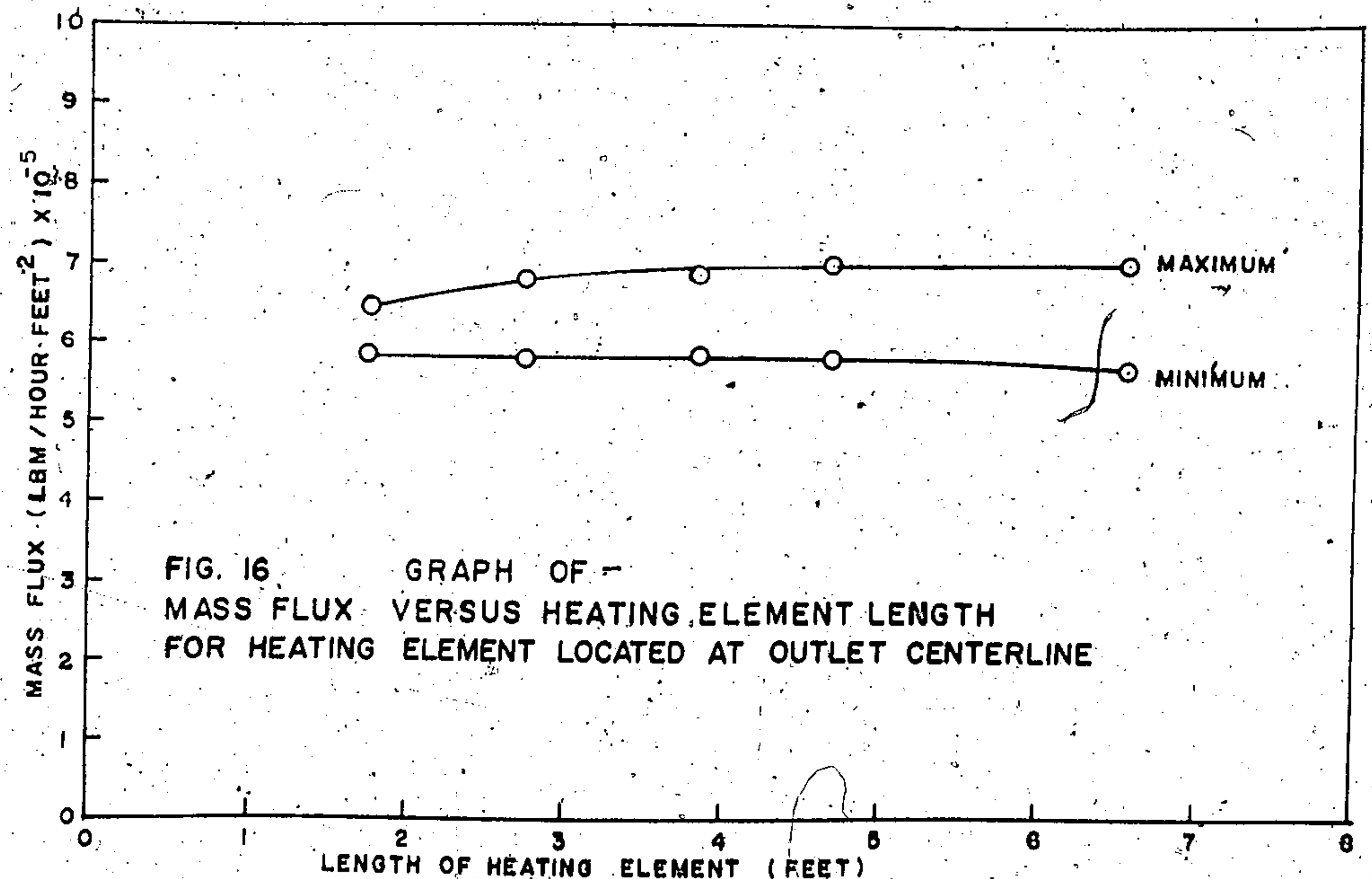

FIG. 16 GRAPH OF —
MASS FLUX VERSUS HEATING ELEMENT LENGTH
FOR HEATING ELEMENT LOCATED AT OUTLET CENTERLINE

FIGURE 16

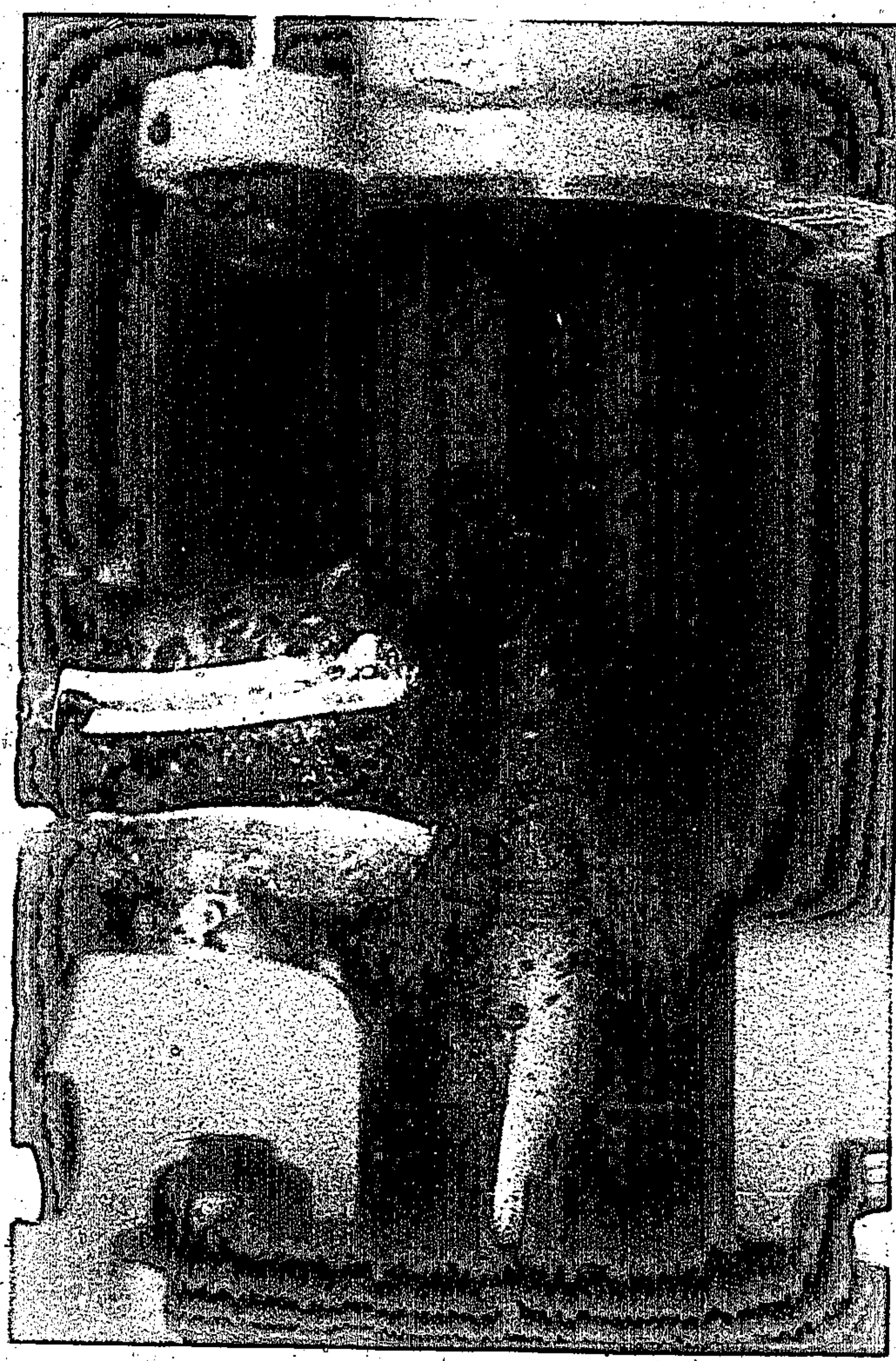

FIG. 17

PHOTOGRAPH OF VOID ATTACHMENT TO A HEAT INPUT SECTION JOINT

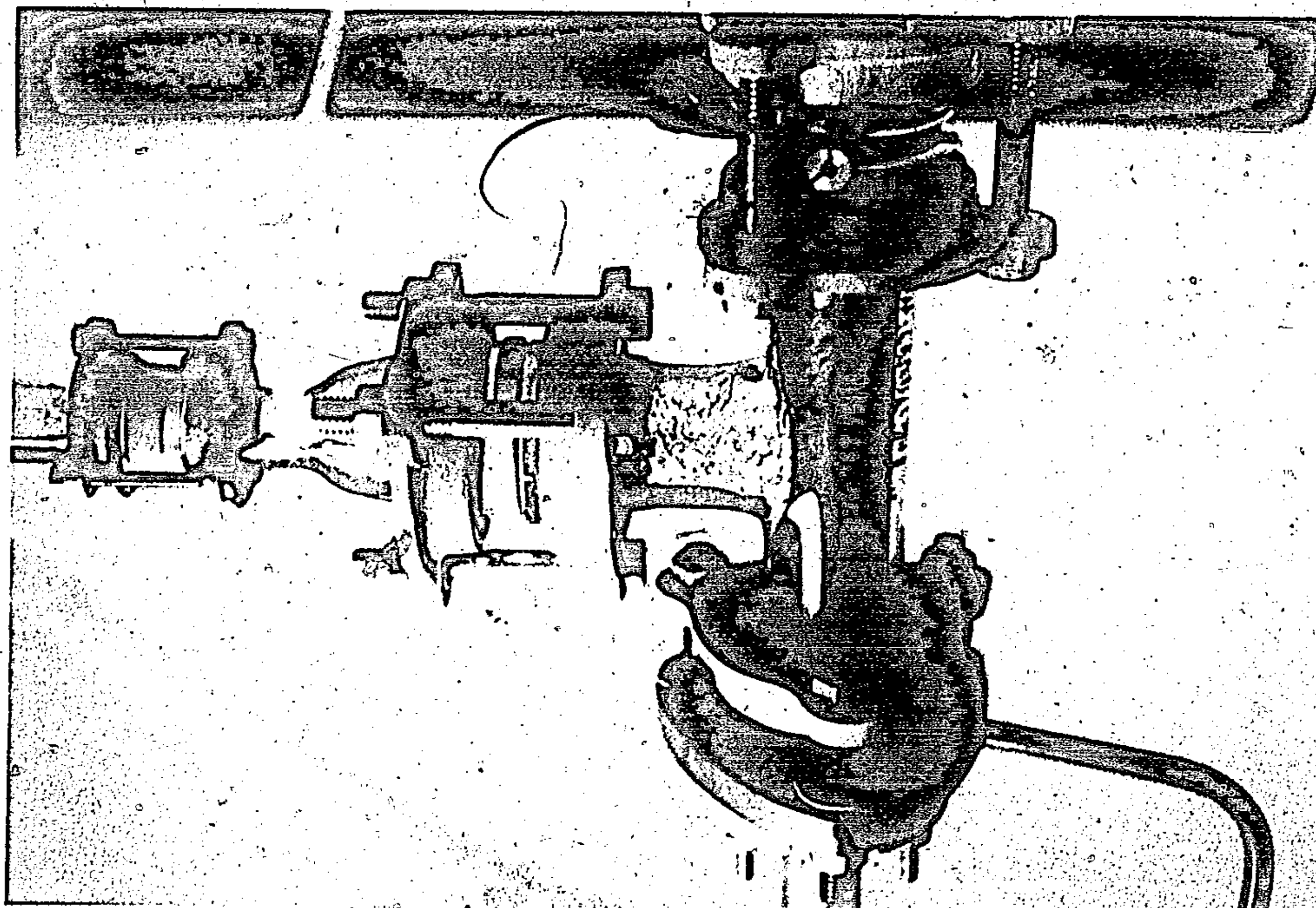

FIG. 18
PHOTOGRAPH OF LARGE VOID FORMATION IN THE SIDE BRANCH OF THE HEAT INPUT SECTION OUTLET "TEE"

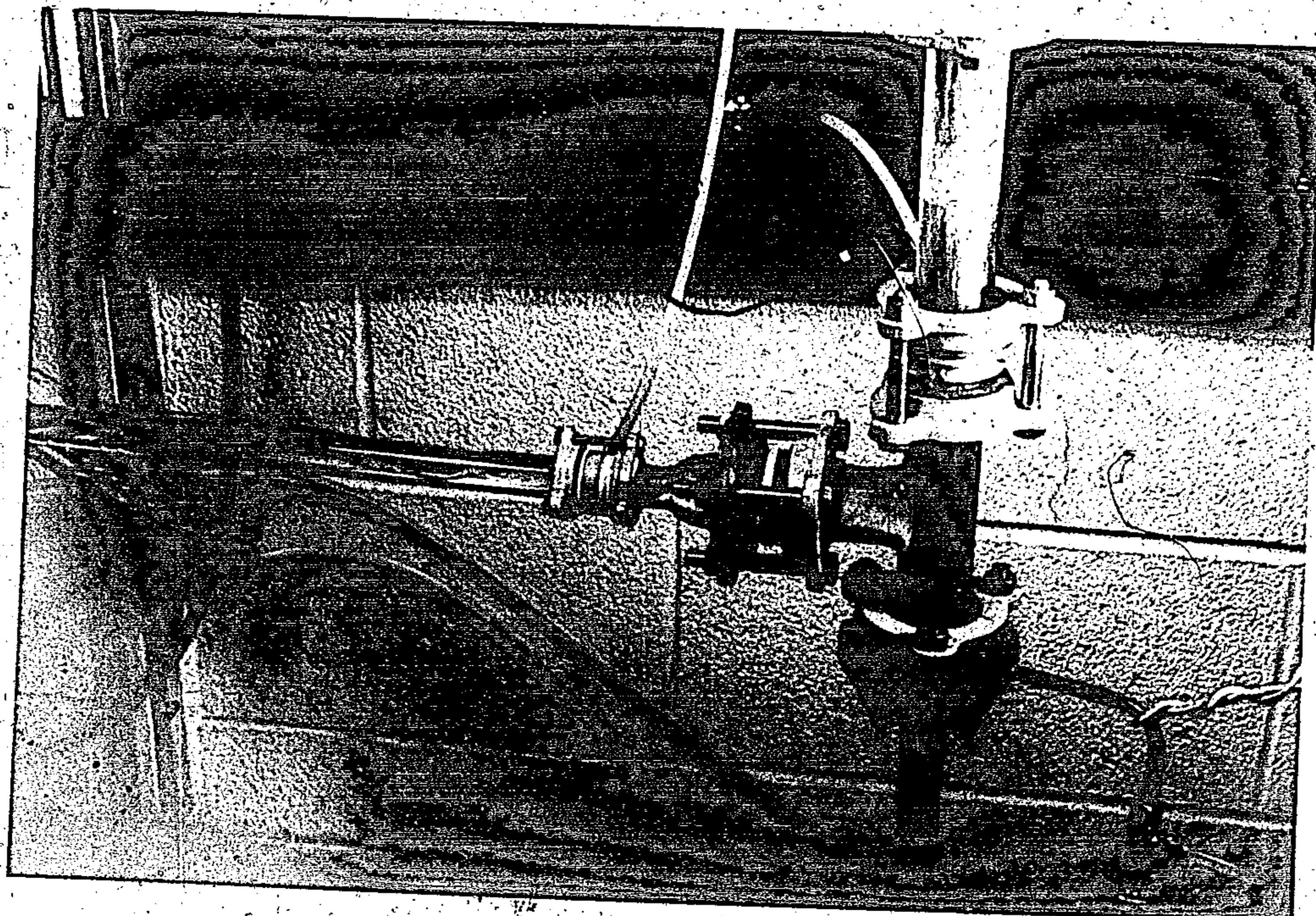

FIG. 19

PHOTOGRAPH OF SINGLE HELICAL VAPOUR TUBE IN
HORIZONTAL CONNECTING SECTION

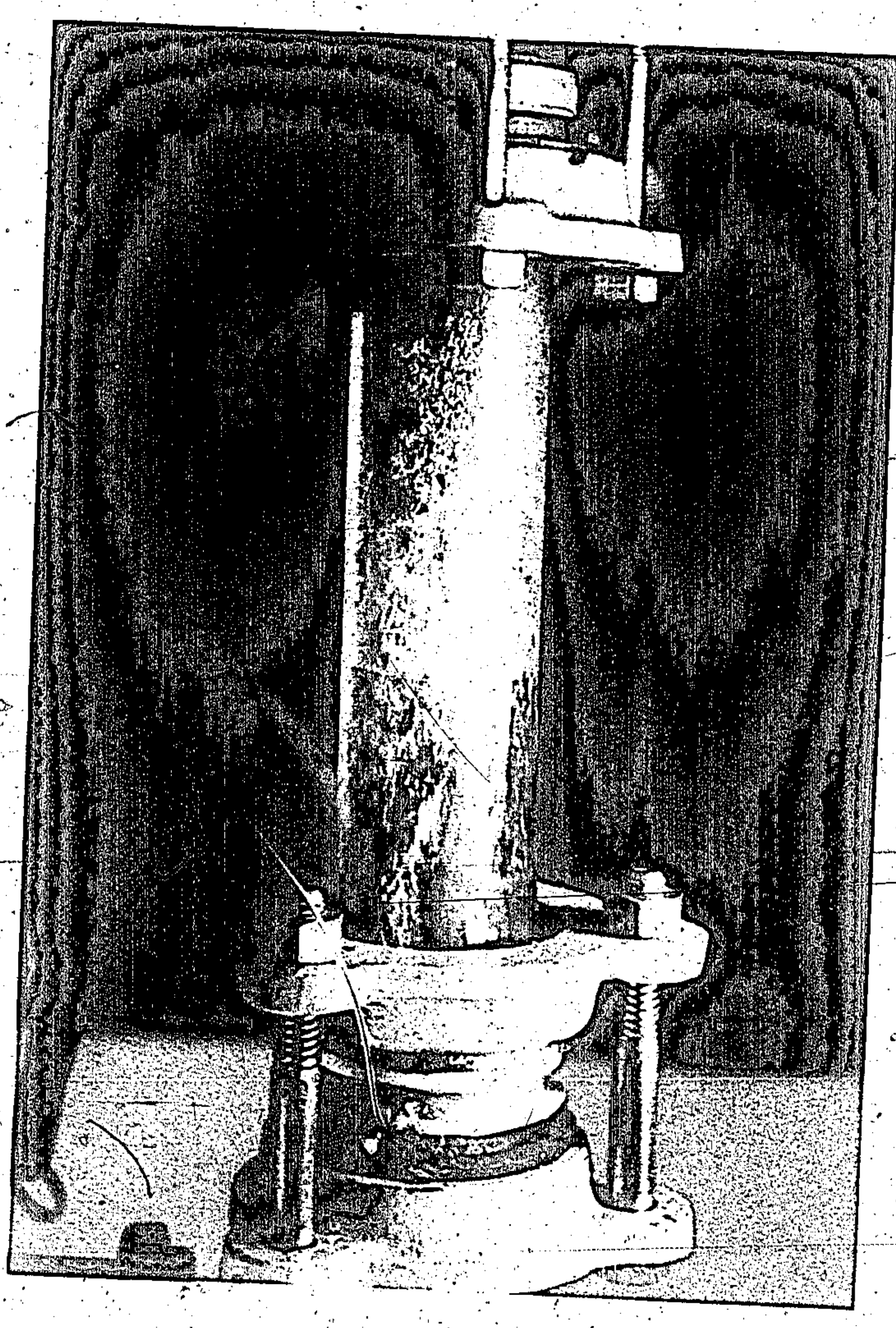

FIG. 20

PHOTOGRAPH OF DRYOUT OF HEATING TUBE SURFACE tube which can be seen in the horizontal section. This too is another possible flow configuration indicating that maximum heat input has been reached. In fact, it is quite possible to observe twin helical vapour tubes which may exist side by side in the horizontal section but which may never join until they reach the inlet tee of the riser section.

One last piece of information remains to be discussed and that is the mode of flashing in the riser. During the orifice plate tests it was observed that the joints in the riser seemed to provide nucleation sites for flashing of the fluid. This same observation was made for all tests concerned with the heaters.

The flash point in the riser always jumped from one joint to the next. Subsequent tests of the system with larger riser diameters have proven that a completely smooth walled riser devoid of joints or projections has a detrimental effect on the operation of the thermosiphon. In fact a string of disks were suspended in the larger risers and these did allow flashing to take place and also lowered the minimum heat input limit. Consequently it is felt that the reason that the minimum thermosiphon operating limit is constant for all heaters regardless of their position is because of the particular geometry used which put the last joint which could act as a flash initiator 5.3 feet below the riser outlet.

13

V MODEL

A simple mathematical model for the two phase reversed flow thermosiphon was postulated for the prediction of the maximum and minimum performance of the loop.

The assumptions incorporated into the model are:

1. At all riser locations where vapour is present the flow is considered to be homogeneous with no slip between the liquid and vapour phases. Such mixtures have the kinematic viscosity of the non-flashing liquid and a density based on an empirical variation of void fraction between zero at the flash point to a maximum at the exit of the riser, the maximum void fraction being determined by the quality at the outlet of the riser. The flash point locations used for the prediction of maximum and minimum performance are those which have been recorded as observed during the experimentation.

2. A constant heat input per unit heater length was assumed.

3. No boiling occurs in the heat input annulus.

4. There is no heat transfer from the loop to the surrounding atmosphere.

The computation of the flow rate is accomplished by evaluating separately the static pressures around the loop and the frictional pressure losses due to the moving fluid. Thus the fluid will be treated as being inviscid for the calculations of the static pressure at the bottom of the heat of the heat input section and the bottom of the riser section.

The calculation of the static pressure at the bottom of the heat input section is an iterative procedure consisting of the following steps:

1. Assuming the heater section outlet temperature is equation to the inlet temperature calculate the frictionless flow static pressure at the bottom of the heater section due to the head of liquid.

2. Assume that the temperature of the bottom of the heater section is the saturation temperature for the static pressure calculated.

3. Recalculate the inviscid flow static pressure rise through the downflow tube using the expression

$$P_{HI} - P_{reservoir} = \frac{g}{g_c}[(L_T - L_H)\rho_{tin} + L_H\ \rho[(t_{in} + t_{out})/2]]\ lbf/ft^2$$

Eqn. 11

4. Repeat steps 2 and 3 until there is negligible change in the static pressure rise.

The next part of the calculation is concerned with determining the inviscid flow, static pressure drop through the riser. The pressure drop along the non-flashing portion of the riser is given by:

$$\Delta P_{NF} = \rho_{out}\ \frac{g}{g_c}\ (L_T - y) \qquad \text{Eqn. 12}$$

where y is the length of the flashing column of liquid in the riser.

The static pressure drop along the flashing portion of the riser is determined as follows:

The riser exit quality, X_{exit}, is given by,

$$X_{exit} = \frac{h_{out} - h_{L\ sat\ exit}}{h_{fg\ exit}} \qquad \text{Eqn. 13}$$

For no slip

$$\alpha_{exit} = \frac{V_{g\ exit}}{\left(\frac{1-X_{exit}}{X_{exit}}\right) V_{L\ exit} + V_{g\ exit}} \qquad \text{Eqn. 14}$$

Let the mean void fraction over the flashing region be

$$\alpha_{mean} = N\,\alpha_{exit} \quad (0 \leq N \leq 1) \qquad \text{Eqn. 15}$$

where N is an empirical weighting factor which is introduced to compensate for the fact that the void fraction varies from 0 to α_{exit}, there is slip between the two phases, and the fluid does not behave as a homogeneous liquid.

Then the static pressure drop over the flashing portion of the riser is

$$\Delta P_F = y\,\rho_{L\ sat\ exit}\,\frac{g}{g_c}\,(1 - N\,\alpha_{exit}) \qquad \text{Eqn. 16}$$

and the static pressure drop over the entire riser section is given by,

$$P_{BR} - P_{reservoir} = \Delta P_{NF} + \Delta P_F = \frac{g}{g_c}\left[(L_T - y)\rho_{out} + y\rho_{L\ sat\ exit}(1-\alpha_{mean})\right] \text{lbf/ft}^2 \qquad \text{Eqn. 17}$$

After determination of the static pressure rise and pressure drop, the difference between the two values or the frictional pressure drop is used to solve for the volume flow rate $\dot{Q}$ according to the expression

$$\dot{Q} = \sqrt{\frac{P_{HI} - P_{BR}}{\rho_{in}} \quad \frac{2g_c}{\Sigma\ K_i/A_i^2}} \quad ft^3/sec \qquad \text{Eqn. 18}$$

where the $\Sigma\ K_i/A_i^2$ term takes into account the summation of all friction losses through the expansions, contractions, elbows, tees, and fluid friction in the tubing. The pipe loss coefficient K is equal to fL/D.

The mass flow rate is given by:

$$\dot{m} = \rho\ \dot{Q}\ \text{lbm/sec} \qquad \text{Eqn. 19}$$

The method used to obtain initial estimates of the friction factors was accomplished by using Eqn. 1 and the minimum Froude Number limit of 0.31 for determining an estimate of flow velocity and consequently Reynolds Number for the heat input section which then makes estimates for the rest of the flow loop possible.

By using the results of the flow rate calculation to determine new estimates of the friction factors around the loop an alerative process can be undertaken to refine the value of the flow rate. The flash point saturation temperature was then calculated from the static pressure at the flash point in the riser. This temperature was then used as the outlet temperature from the heat input section and all the preceeding calculations starting with Eqn. 11 were repeated until there were negligible changes in the values being determined.

In order to evaluate the capability of the model the following properties and geometric data were used to determine the maximum and minimum performance for the chosen heater length.

Working Fluid	-	Freon 113
Condenser Pressure	-	Atmospheric
Heater Length (L_H)	-	4.0 feet
Total Head of fluid (L_T)	-	13.1 feet
T_{in}	-	110.2°F (max); 115.3°f (min)
y	-	10.0 feet (max); 5.3 feet (min)

The friction loss coefficients are given for the standard geometry used.

Thermosiphon Section	K_i/A_i^2 maximum value	$(1/ft^4)$ minimum value
2 inch Tee	3782	3782
8 inches of 2 inch I.D. pipe	124	129
Sudden Contraction	11766	11766
13 inches of 1 inch I.D. pipe	5637	5812
1 inch Elbow	20169	20169
6 inches of 1 inch I.D. pipe	2602	2683
Sudden Contraction	92307	92307
Conical Enlargement	39978	39978
4 inches of 1 inch I.D. pipe	1735	1788
1 inch Tee	315414	315414
Sudden Contraction	175230	15463
11 feet Annular Pipe	1323055	1360064
1 inch Tee	315414	315414
Sudden Expansion	175230	175230
Sudden Contraction	59403	59403
28 inches 5/8 I.D. Pipe	117293	121236
5/8 inch T.	396023	396023
13 feet 5/8 inch pipe	658518	675457
Sudden Expansion	176010	176010
40 inches 2 inch I.D. pipe	618	643
2 inch Tee	3782	3782
$\Sigma K_i/A_i^2$	3878624	3952320

All friction factors were calculated from pipe flow data using experimentally determined Reynolds Numbers. The annulus was treated as a round pipe with diameter equal to the equivalent diameter of the annulus. By matching the experimental data to the model predictions, it was determined that a value of N = .185 gave the best overall simulation.

A comparison of the limiting flow rates and power inputs predicted by the model with the corresponding observed values in the thermosiphon are shown in Table 5 which also includes a maximum flow rate prediction if the riser is completely full of two phase liquid and a comparison of the predictions of minimum flow rate by the model, Bonilla's method and the limiting Froude Number Method.

TABLE 5

Comparison of Results

Heater Length 48 inches

Length of Flashing Column y	Observed		Predicted N = 0.185		Value of N for agreement of $\dot{m}$	Predicted Q_{in}
	$\dot{m}$	Q_{in}	$\dot{m}$	Q_{in}		
5.3 feet	.400 lbm/sec	4,222 Btu/hr	.373 lbm/sec	3,712 Btu/hr	.215	3,881 Btu/hr
10.0 feet	.470 lbm/sec	10,078 Btu/hr	.512 lbm/sec	10,480 Btu/hr	.154	9,815 Btu/hr

Model Predicted Maximum Flow Rate .576 lbm/sec

Model Predicted Minimum Flow Rate .099 lbm/sec

Bonilla's Predicted Minimum Flow Rate .105 lbm/sec

Froude Number Predicted Minimum Flow Rate .207 lbm/sec

VI CONCLUSIONS

The following conclusions have been reached after studying the results of the experiments:

1. A flash initiator mechanism of some type must be present in the riser to ensure that stable flashing does occur. In the absence of suitable nucleation sites the liquid becomes superheated because no boiling takes place. This is an unstable condition which increases in severity as the superheat increases until a condition where spontaneous flashing is reached. This situation creates large fluctuations in the flash point position and hinders stable reversed flow operation.

2. As indicated by the reduced values of maximum performance for the short heaters; there exists a lower limit on heater length below which boiling reversed flow cannot be attained. The maximum performance is lower because of the high heat flow rate per unit of heating surface area. The working fluid is not capable of handling this high heat flux without large amounts of void being formed. The presence of void in the heat input section produces a bouyancy force which acts to retard the flow before more flashing generates a larger bouyancy force in the riser section. Thus the shorter the heater, the sooner it produces the large amounts of void which act to reverse the flow and consequently the lower the maximum performance of the system.

3. For long heaters, heater length and position have little effect on the maximum performance of the thermosiphon which indicates that the bouyancy forces in the heat input section are negligible when compared with those produced in the riser section due to flashing.

4. For long heaters the mechanism of reversal is slightly different from that of the short heaters. In this case the maximum bouyancy force and consequently flow rate has been generated by flashing in the riser section. Any increase in heat input does not increase the amount of flashing or the flow rate beyond this limit but it does increase the amount of void present in the heat input section. As this happens the bouyancy forces generated in the heat input section oppose the increase in flow rate and presently cause a reversal.

5. For heaters longer than the minimum length discussed in the results chapter; the minimum performance of the thermosiphon is not a function of heater length or position because the only factor governing it is the bouyancy force generated by the flashing in the riser section. As the flash point temperature approaches the saturation temperature corresponding to the pressure in the condenser the differences become so small that if the fluid for some reason superheats, it may be swept into the reservoir before it flashes. Once this has occurred the bouyancy force driving the flow is gone and because heating is continuous in the heat input section the bouyancy forces generated there will favour natural convection,

thus reversing the flow direction.

In addition several conclusions become evident from studying the information provided by the model. These are:

1. Since the friction losses are a function of pipe diameter it should be possible to increase the flow rate by increasing the flow areas of the riser and heat input sections.

2. The variation in weighting factor N necessary to match the observed flow rates to the predicted values indicates that the rate of increase in void fraction per unit length of riser is not the same for the two performance limits. If the model is correct it would seem that the amount of void per unit length increases faster for lower power inputs than it does for higher power inputs. This is indicated by the larger value of N for the minimum performance limit determined for the four foot heater.

Finally it may be stated that although the reversed flow, boiling thermosiphon is operating in a metastable condition so that by exceeding either of its operating limits or altering drastically one of its variables, a reversal in flow direction takes place; it is a functional system which can be used in situations where it is necessary to have only subcooled boiling and no continuous external pumping of the working fluid.

APPENDIX I

PROPERTIES OF REFRIGERANT (FREON) 113

REFRIGERANT 113
TRICHLOROTRIFLUOROETHANE

Chemical Formula	$CCl_2F\text{-}CClF_2$
Molecular Weight	187.39
Boiling Temperature at Atmospheric Pressure, F	117.6
Freezing Temperature at Atmospheric Pressure, F	-31
Critical Temperature, F	417.4
Critical Pressure, psia	498.9
Critical Density, lb per cu ft	36.0
Density of Liquid at 86 F, lb per cu ft	96.96
Specific Volume of Saturated Vapor at 5 F, cu ft per lb	27.04
Specific Heat of Liquid at 86 F, Btu per (lb) (F)	0.218
Specific Heat Ratio (c_p/c_v) of Vapor at 86 F and One Atmosphere Pressure	1.12
Thermal Conductivity, (Btu) (ft) per (sq ft) (hr) (F):	
Saturated Liquid at 5 F	0.044
Saturated Liquid at 86 F	0.037
Vapor at Saturation Pressure at 5 F	0.0035
Vapor at 1/2 Atmosphere Pressure at 86 F	0.0045
Viscosity, Centipoises:	
Saturated Liquid at 5 F	1.28
Saturated Liquid at 86 F	0.638
Vapor at Saturation Pressure at 5 F	0.0079
Vapor at 1/2 Atmosphere Pressure at 86 F	0.0096
Relative Dielectric Strength of Vapor at 77 F and 0.4 Atmosphere Pressure (Nitrogen = 1)	3.9
Color	Clear and colorless
Odor and Detection	Faint ethereal odor. Leaks readily located with a halide leak detector.
Flammability	Nonflammable
Toxicity, Underwriters' Laboratories Classification	Much less than Group 4, but more than Group 5

TABLE 9 . . . PROPERTIES OF LIQUID AND SATURATED VAPOR† — REFRIGERANT 113

TEMP F	PRESSURE lb per sq in		VOLUME cu ft per lb		DENSITY lb per cu ft		ENTHALPY ** Btu per lb			ENTROPY ** Btu per (lb) (°R)		TEMP F
t	Absolute p	Gage p	Liquid v_f	Vapor v_g	Liquid $1/v_f$	Vapor $1/v_g$	Liquid h_f	Latent h_{fg}	Vapor h_g	Liquid s_f	Vapor s_g	t
-30	0.2987	29.31*	0.00947	82.26	105.64	0.01216	1.97	72.68	74.65	0.0047	0.1738	-30
-28	0.3214	29.27*	.00948	76.81	105.50	.01302	2.36	72.57	74.93	.0056	.1737	-28
-26	0.3458	29.22*	.00949	71.71	105.37	.01395	2.76	72.45	75.21	.0065	.1736	-26
-24	0.3718	29.16*	.00950	66.99	105.23	.01493	3.16	72.33	75.49	.0074	.1735	-24
-22	0.3995	29.11*	.00952	62.63	105.09	.01597	3.56	72.21	75.77	.0083	.1733	-22
-20	0.4288	29.05*	0.00953	58.61	104.96	0.01706	3.96	72.09	76.05	0.0092	0.1732	-20
-18	0.4600	28.98*	.00954	54.88	104.82	.01822	4.36	71.98	76.34	.0101	.1731	-18
-16	0.4931	28.92*	.00955	51.42	104.68	.01945	4.76	71.86	76.62	.0110	.1730	-16
-14	0.5280	28.85*	.00957	48.23	104.54	.02074	5.16	71.74	76.90	.0119	.1729	-14
-12	0.5652	28.77*	.00958	45.25	104.40	.02210	5.56	71.62	77.18	.0128	.1729	-12
-10	0.6046	28.69*	0.00959	42.48	104.26	0.02354	5.96	71.51	77.47	0.0137	0.1728	-10
- 8	0.6462	28.60*	.00960	39.92	104.12	.02505	6.36	71.39	77.75	.0146	.1727	- 8
- 6	0.6902	28.51*	.00962	37.54	103.98	.02664	6.76	71.27	78.03	.0155	.1726	- 6
- 4	0.7369	28.42*	.00963	35.31	103.84	.02832	7.17	71.15	78.32	.0164	.1726	- 4
- 2	0.7860	28.32*	.00964	33.24	103.70	.03009	7.57	71.03	78.60	.0173	.1725	- 2
0	0.8377	28.21*	0.00966	31.31	103.56	0.03194	7.98	70.92	78.89	0.0182	0.1725	0
2	0.8924	28.10*	.00967	29.52	103.41	.03388	8.38	70.80	79.18	.0190	.1724	2
4	0.9503	27.99*	.00968	27.84	103.27	.03592	8.78	70.68	79.46	.0199	.1724	4
5	0.9802	27.92*	.00969	27.04	103.20	.03698	8.98	70.62	79.60	.0203	.1723	5
6	1.011	27.86*	.00970	26.27	103.13	.03806	9.19	70.56	79.75	.0208	.1723	6
8	1.075	27.73*	.00971	24.81	102.98	.04031	9.59	70.44	80.03	.0216	.1723	8
10	1.142	27.60*	0.00972	23.45	102.84	0.04265	10.00	70.32	80.32	0.0225	0.1723	10
12	1.213	27.45*	.00974	22.17	102.69	.04511	10.41	70.20	80.61	.0234	.1722	12
14	1.288	27.30*	.00975	20.97	102.55	.04769	10.81	70.08	80.89	.0242	.1722	14
16	1.366	27.14*	.00977	19.84	102.40	.05040	11.22	69.96	81.18	.0251	.1722	16
18	1.448	26.97*	.00978	18.79	102.25	.05322	11.62	69.84	81.46	.0259	.1722	18
20	1.534	26.80*	0.00979	17.81	102.10	0.05616	12.03	69.72	81.75	0.0268	0.1722	20
22	1.624	26.61*	.00981	16.89	101.96	.05922	12.44	69.60	82.04	.0276	.1721	22
24	1.719	26.42*	.00982	16.02	101.81	.06243	12.85	69.48	82.33	.0285	.1721	24
26	1.818	26.22*	.00984	15.20	101.66	.06579	13.26	69.36	82.62	.0293	.1722	26
28	1.922	26.01*	.00985	14.43	101.51	.06929	13.67	69.24	82.91	.0302	.1722	28
30	2.031	25.79*	0.00987	13.71	101.36	0.07294	14.08	69.12	83.20	0.0310	0.1722	30
32	2.145	25.55*	.00988	13.03	101.21	.07675	14.49	69.00	83.49	.0318	.1722	32
34	2.264	25.31*	.00990	12.39	101.06	.08071	14.91	68.87	83.78	.0327	.1722	34
36	2.388	25.06*	.00991	11.79	100.91	.08483	15.32	68.75	84.07	.0335	.1722	36
38	2.519	24.79*	.00993	11.22	100.76	.08913	15.74	68.62	84.36	.0343	.1722	38
40	2.655	24.52*	0.00994	10.68	100.60	0.09361	16.16	68.50	84.65	0.0352	0.1723	40
42	2.797	24.23*	.00996	10.18	100.45	.09826	16.57	68.37	84.94	.0360	.1723	42
44	2.944	23.93*	.00997	9.703	100.30	.1031	16.99	68.25	85.24	.0368	.1723	44
46	3.098	23.61*	.00999	9.253	100.14	.1081	17.41	68.12	85.53	.0377	.1724	46
48	3.258	23.29*	.01000	8.830	99.99	.1133	17.82	68.00	85.82	.0385	.1724	48
50	3.427	22.94*	0.01002	8.426	99.83	0.1187	18.24	67.87	86.11	0.0393	0.1725	50
52	3.602	22.59*	.01003	8.044	99.68	.1243	18.66	67.74	86.40	.0401	.1726	52
54	3.784	22.22*	.01005	7.682	99.52	.1302	19.08	67.61	86.69	.0410	.1726	54
56	3.973	21.83*	.01006	7.342	99.37	.1362	19.50	67.48	86.98	.0418	.1727	56
58	4.170	21.43*	.01008	7.018	99.21	.1425	19.93	67.35	87.28	.0426	.1727	58
60	4.374	21.02*	0.01010	6.713	99.05	0.1490	20.35	67.22	87.57	0.0434	0.1728	60
62	4.586	20.59*	.01011	6.424	98.89	.1557	20.77	67.09	87.86	.0442	.1729	62
64	4.807	20.14*	.01013	6.149	98.73	.1626	21.19	66.96	88.15	.0450	.1729	64
66	5.036	19.67*	.01015	5.889	98.58	.1698	21.62	66.83	88.45	.0459	.1730	66
68	5.275	19.18*	.01016	5.640	98.42	.1773	22.05	66.69	88.74	.0467	.1731	68
70	5.523	18.68*	0.01018	5.404	98.26	0.1851	22.48	66.56	89.04	0.0475	0.1731	70
72	5.780	18.16*	.01019	5.180	98.10	.1931	22.90	66.43	89.33	.0483	.1732	72
74	6.042	17.62*	.01021	4.971	97.93	.2012	23.33	66.29	89.62	.0491	.1733	74
76	6.320	17.06*	.01023	4.769	97.77	.2097	23.76	66.16	89.92	.0499	.1734	76
78	6.607	16.47*	.01025	4.574	97.61	.2186	24.19	66.02	90.21	.0507	.1735	78
80	6.902	15.87*	0.01026	4.392	97.45	0.2277	24.63	65.88	90.51	0.0515	0.1736	80
82	7.208	15.25*	.01028	4.218	97.28	.2371	25.06	65.74	90.80	.0523	.1737	82
84	7.527	14.60*	.01030	4.051	97.12	.2468	25.49	65.60	91.09	.0531	.1738	84
86	7.856	13.93*	.01031	3.893	96.96	.2569	25.93	65.46	91.39	.0539	.1739	86
88	8.194	13.24*	.01033	3.742	96.79	.2672	26.36	65.32	91.68	.0547	.1740	88
90	8.545	12.53*	0.01035	3.600	96.63	0.2778	26.80	65.18	91.98	0.0555	0.1741	90
92	8.908	11.79*	.01037	3.463	96.46	.2868	27.24	65.04	92.28	.0563	.1742	92
94	9.281	11.03*	.01039	3.333	96.30	.3001	27.67	64.90	92.57	.0571	.1743	94
96	9.668	10.24*	.01040	3.208	96.13	.3117	28.11	64.75	92.86	.0578	.1744	96
98	10.07	9.42*	0.01042	3.089	95.96	0.3237	28.55	64.60	93.15	0.0586	0.1745	98

† From published data (1938) of E. I. du Pont de Nemours & Co., Inc. Used by permission.
* Inches of mercury below one standard atmosphere.
** Based on zero for the saturated liquid at -40 F.

TABLE 9 . . . PROPERTIES OF LIQUID AND SATURATED VAPOR (continued)

TEMP F	PRESSURE lb per sq in		VOLUME cu ft per lb		DENSITY lb per cu ft		ENTHALPY** Btu per lb			ENTROPY** Btu per (lb) (°R)		TEMP F
t	Absolute p	Gage p_g	Liquid v_f	Vapor v_g	Liquid $1/v_f$	Vapor $1/v_g$	Liquid h_f	Latent h_{fg}	Vapor h_g	Liquid s_f	Vapor s_g	t
100	10.48	8.59*	0.01044	2.976	95.79	0.3360	28.99	64.46	93.45	0.0594	0.1746	100
102	10.91	7.71*	.01046	2.867	95.63	0.3488	29.44	64.31	93.75	.0602	.1747	102
104	11.35	6.82*	.01048	2.762	95.46	0.3620	29.89	64.16	94.05	.0610	.1748	104
106	11.81	5.88*	.01050	2.662	95.29	0.3756	30.33	64.01	94.34	.0618	.1750	106
108	12.28	4.93*	.01051	2.567	95.12	0.3896	30.78	63.86	94.64	.0626	.1751	108
110	12.76	3.95*	0.01053	2.477	94.95	0.4038	31.22	63.71	94.93	0.0634	0.1752	110
112	13.25	2.95*	.01055	2.391	94.78	0.4182	31.67	63.56	95.23	.0641	.1753	112
114	13.76	1.91*	.01057	2.308	94.61	0.4333	32.12	63.40	95.52	.0649	.1755	114
116	14.29	0.83*	.01059	2.228	94.43	0.4489	32.57	63.25	95.82	.0657	.1756	116
118	14.84	0.14	.01061	2.151	94.26	0.4649	33.03	63.09	96.12	.0665	.1757	118
120	15.40	0.70	0.01063	2.078	94.09	0.4813	33.48	62.93	96.41	0.0673	0.1758	120
122	15.97	1.27	.01065	2.008	93.92	0.4981	33.93	62.78	96.71	.0680	.1760	122
124	16.56	1.86	.01067	1.941	93.74	0.5153	34.38	62.62	97.00	.0688	.1761	124
126	17.17	2.47	.01069	1.876	93.57	0.5330	34.83	62.46	97.29	.0696	.1763	126
128	17.80	3.10	.01071	1.814	93.39	0.5514	35.29	62.30	97.59	.0704	.1764	128
130	18.45	3.74	0.01073	1.754	93.22	0.5702	35.75	62.14	97.89	0.0712	0.1765	130
132	19.11	4.41	.01075	1.697	93.04	0.5894	36.21	61.97	98.18	.0719	.1767	132
134	19.79	5.09	.01077	1.642	92.86	0.6091	36.67	61.80	98.47	.0727	.1768	134
136	20.48	5.78	.01079	1.590	92.69	0.6290	37.13	61.64	98.77	.0735	.1770	136
138	21.19	6.49	.01081	1.540	92.51	0.6494	37.59	61.48	99.06	.0742	.1771	138
140	21.93	7.23	0.01083	1.491	92.33	0.6707	38.05	61.31	99.36	0.0750	0.1773	140
142	22.69	7.99	.01085	1.444	92.15	0.6926	38.52	61.13	99.65	.0758	.1774	142
144	23.47	8.77	.01087	1.399	91.98	0.7150	38.98	60.96	99.94	.0765	.1775	144
146	24.27	9.57	.01089	1.355	91.80	0.7379	39.45	60.79	100.24	.0773	.1777	146
148	25.09	10.39	.01092	1.313	91.62	0.7615	39.92	60.61	100.53	.0781	.1778	148
150	25.93	11.23	0.01094	1.273	91.44	0.7856	40.38	60.44	100.82	0.0789	0.1780	150
152	26.79	12.09	.01096	1.234	91.25	0.8102	40.85	60.27	101.11	.0796	.1782	152
154	27.67	12.97	.01098	1.197	91.07	0.8353	41.32	60.09	101.41	.0804	.1783	154
156	28.56	13.86	.01100	1.162	90.89	0.8608	41.79	59.91	101.70	.0812	.1785	156
158	29.48	14.78	0.01102	1.128	90.71	0.8869	42.26	59.73	101.99	0.0819	0.1786	158
160	30.44	15.74	0.01105	1.094	90.53	0.9141	42.74	59.55	102.29	0.0827	0.1788	160
170	35.53	20.83	0.01116	0.9442	89.60	1.059	45.12	58.62	103.74	0.0865	0.1796	170
180	41.22	26.52	0.01128	0.8193	88.67	1.221	47.53	57.66	105.19	0.0903	0.1804	180
190	47.60	32.90	0.01140	0.7134	87.72	1.402	49.97	56.66	106.63	0.0940	0.1813	190
200	54.66	39.96	0.01153	0.6241	86.76	1.602	52.45	55.62	108.07	0.0978	0.1821	200
210	62.50	47.80	0.01166	0.5477	85.79	1.826	54.96	54.54	109.50	0.1015	0.1830	210
220	71.07	56.37	0.01179	0.4827	84.80	2.072	57.49	53.43	110.92	0.1052	0.1839	220
250	101.8	87.1	0.0122	0.339	81.71	2.953	62.87	51.01	113.88	0.1123	0.1842	250
300	175.6	161.	0.0132	0.190	75.63	5.272	75.82	44.33	120.15	0.1297	0.1881	300
350	283.3	269.	0.0147	0.105	67.80	9.489	90.12	34.68	124.80	0.1477	0.1905	350
360	309.8	295.	0.0152	0.093	65.98	10.708	92.98	32.40	125.38	0.1511	0.1906	360
370	338.0	323.	0.0156	0.081	63.94	12.383	96.50	29.14	125.64	0.1564	0.1915	370
380	368.1	353.	0.0163	0.069	61.50	14.47	99.66	25.52	125.18	0.1589	0.1893	380
390	400.1	385.	0.0171	0.059	58.58	17.00	102.91	21.52	124.43	0.1627	0.1880	390
400	434.3	420.	0.0182	0.049	55.02	20.54	105.78	16.84	122.62	0.1659	0.1855	400
410	470.6	456.	0.0199	0.039	50.21	26.11	108.34	10.32	118.66	0.1688	0.1807	410
417.4	498.9	484.	0.028	0.028	35.96	35.96	109.49	00.00	109.49	0.1699	0.1699	417.4

*Inches of mercury below one standard atmosphere.

TABLE 10...PROPERTIES OF SUPERHEATED VAPOR (continued)

Temp F	Abs Pressure 8.0 psi Gage Pressure 13.64 in. Vac (Sat'n Temp 86.9 F)			Abs Pressure 9.0 psi Gage Pressure 11.60 in. Vac (Sat'n Temp 92.5 F)			Abs Pressure 10.0 psi Gage Pressure 9.57 in. Vac (Sat'n Temp 97.6 F)			Abs Pressure 11 psi Gage Pressure 7.53 in. Vac (Sat'n Temp 102.4 F)		
t	v	h	s	v	h	s	v	h	s	v	h	s
(Sat'n)	(3.828)	(91.52)	(0.1739)	(3.431)	(92.35)	(0.1742)	(3.110)	(93.11)	(0.1745)	(2.845)	(93.81)	(0.1747)
90	3.850	92.01	0.1748	....	....	....	....	....	....	....	....	....
100	3.924	93.56	0.1776	3.481	93.52	0.1763	3.124	93.48	0.1751	....	....	....
110	3.999	95.12	.1804	3.547	95.08	.1791	3.183	95.04	.1779	2.887	95.01	0.1769
120	4.073	96.69	.1831	3.613	96.66	.1819	3.242	96.62	.1806	2.941	96.58	.1796
130	4.147	98.28	.1858	3.679	98.25	.1846	3.301	98.21	.1834	2.995	98.17	.1823
140	4.221	99.[illegible]	.1885	3.745	99.84	.1872	3.361	99.81	.1860	3.049	99.77	.1850
150	4.295	101.48	0.1912	3.810	101.45	0.1899	3.420	101.41	0.1887	3.103	101.38	0.1877
160	4.369	103.10	.1938	3.874	103.07	.1925	3.480	103.03	.1914	3.157	103.00	.1903
170	4.442	104.74	.1964	3.940	104.70	.1951	3.539	104.66	.1940	3.211	104.63	.1929
180	4.515	106.38	.1990	4.004	106.34	.1977	3.595	106.31	.1966	3.265	106.28	.1955
190	4.588	108.04	.2016	4.070	108.00	.2003	3.658	107.96	.1991	3.319	107.93	.1981
200	4.661	109.71	0.2041	4.135	109.67	0.2028	3.716	109.63	0.2017	3.373	109.60	0.2006
210	4.734	111.38	.2066	4.199	111.35	.2054	3.774	111.32	.2042	3.426	111.26	.2032
220	4.807	113.07	.2091	4.265	113.04	.2079	3.832	113.01	.2067	3.480	112.97	.2057
230	4.880	114.77	.2116	4.330	114.74	.2104	3.891	114.71	.2092	3.533	114.67	.2082
240	4.952	116.48	.2141	4.395	116.45	.2129	3.950	116.42	.2117	3.586	116.38	.2106
250	5.024	118.20	0.2166	4.460	118.17	0.2153	4.010	118.14	0.2141	3.639	118.10	0.2131
260	5.096	119.93	.2190	4.525	119.91	.2177	4.066	119.87	.2166	3.692	119.84	.2155
270	5.168	121.67	.2214	4.590	121.64	.2201	4.126	121.61	.2190	3.745	121.58	.2179
280	5.240	123.42	.2238	4.656	123.40	.2225	4.185	123.37	.2214	3.798	123.34	.2203
290	5.313	125.19	.2261	4.721	125.17	.2249	4.243	125.15	.2237	3.852	125.12	.2227
300	5.387	126.96	0.2285	4.787	126.96	0.2273	4.302	126.94	0.2261	3.906	126.91	0.2250
310	5.460	128.78	.2309	4.852	128.76	.2296	4.360	128.74	.2285	3.960	128.71	.2274
320	5.533	130.58	.2332	4.918	130.57	.2319	4.419	130.54	.2308	4.014	130.51	.2298
330	5.607	132.40	.2355	4.983	132.39	.2343	4.477	132.36	.2331	4.068	132.33	.2321
340	5.682	134.23	.2378	5.048	134.21	.2366	4.537	134.19	.2354	4.122	134.16	.2344
350	5.756	136.07	0.2401	5.112	136.05	0.2388	4.596	136.03	0.2377	4.175	136.00	0.2367
360	5.830	137.92	.2424	5.178	137.90	.2411	4.656	137.83	.2400	4.229	137.85	.2389
370	5.904	139.78	.2447	5.243	139.76	.2434	4.714	139.74	.2422	4.283	139.71	.2412
380	5.975	141.66	.2470	5.307	141.64	.2456	4.772	141.62	.2445	4.336	141.59	.2434
390	6.047	143.55	.2492	5.372	143.52	.2479	4.829	143.50	.2467	4.389	143.48	.2457
400	....	....	....	5.436	145.41	0.2501	4.887	145.39	0.2489	4.441	145.37	0.2479

Temp F	Abs Pressure 12 psi Gage Pressure 5.50 in. Vac (Sat'n Temp 106.8 F)			Abs Pressure 13 psi Gage Pressure 3.46 in. Vac (Sat'n Temp 111.0 F)			Abs Pressure 14 psi Gage Pressure 1.42 in. Vac (Sat'n Temp 114.9 F)			Abs Pressure 16 psi Gage Pressure 1.3 psi (Sat'n Temp 122.1 F)		
(Sat'n)	(2.624)	(94.46)	(0.1750)	(2.435)	(95.08)	(0.1753)	(2.271)	(95.66)	(0.1755)	(2.004)	(96.72)	(0.1760)
110	2.640	94.97	0.1759	....	....	....	....	....	....	....	....	....
120	2.689	96.55	.1786	2.477	96.51	0.1778	2.291	96.47	0.1770	....	....	....
130	2.738	98.14	.1813	2.522	98.10	.1805	2.334	98.06	.1797	2.034	97.99	0.1782
140	2.788	99.73	.1840	2.567	99.70	.1832	2.377	99.66	.1823	2.072	99.59	.1809
150	2.838	101.34	0.1867	2.613	101.31	0.1858	2.421	101.27	0.1850	2.110	101.20	0.1835
160	2.888	102.97	.1894	2.659	102.94	.1885	2.465	102.90	.1876	2.148	102.83	.1862
170	2.938	104.60	.1920	2.704	104.57	.1911	2.508	104.53	.1902	2.186	104.46	.1888
180	2.987	106.25	.1946	2.749	106.21	.1937	2.550	106.18	.1928	2.224	106.11	.1914
190	3.037	107.90	.1972	2.795	107.87	.1963	2.593	107.84	.1954	2.262	107.77	.1940
200	3.086	109.57	0.1997	2.841	109.54	0.1988	2.635	109.51	0.1980	2.299	109.44	0.1965
210	3.135	111.26	.2022	2.887	111.23	.2013	2.678	111.20	.2005	2.336	111.13	.1991
220	3.184	112.95	.2047	2.933	112.92	.2039	2.720	112.89	.2030	2.374	112.83	.2016
230	3.234	114.65	.2072	2.979	114.62	.2064	2.763	114.59	.2055	2.411	114.53	.2041
240	3.283	116.36	.2097	3.025	116.33	.2088	2.806	116.30	.2080	2.448	116.24	.2065
250	3.332	118.08	0.2121	3.071	118.05	0.2113	2.848	118.02	0.2105	2.486	117.96	0.2090
260	3.382	119.81	.2146	3.117	119.79	.2137	2.890	119.76	.2129	2.523	119.70	.2114
270	3.431	121.55	.2170	3.162	121.53	.2162	2.932	121.50	.2153	2.560	121.45	.2138
280	3.479	123.31	.2194	3.208	123.29	.2186	2.975	123.26	.2177	2.596	123.21	.2162
290	3.528	125.09	.2218	3.254	125.07	.2209	3.018	125.04	.2201	2.633	124.99	.2186
300	3.578	126.88	0.2241	3.300	126.86	0.2232	3.060	126.84	0.2225	2.671	126.78	0.2210
310	3.627	128.68	.2265	3.345	128.66	.2256	3.103	128.64	.2248	2.709	128.58	.2233
320	3.676	130.49	.2288	3.391	130.47	.2279	3.145	130.44	.2271	2.746	130.39	.2257
330	3.725	132.31	.2311	3.436	132.29	.2302	3.187	132.26	.2294	2.783	132.21	.2280
340	3.774	134.14	.2334	3.481	134.12	.2325	3.229	134.09	.2317	2.820	134.04	.2303
350	3.823	135.98	0.2357	3.526	135.96	0.2348	3.271	135.94	0.2340	2.857	135.88	0.2326
360	3.872	137.83	.2380	3.572	137.81	.2371	3.313	137.79	.2363	2.895	137.74	.2349
370	3.922	139.69	.2402	3.617	139.68	.2394	3.355	139.65	.2386	2.932	139.60	.2371
380	3.972	141.57	.2425	3.662	141.56	.2416	3.397	141.52	.2408	2.966	141.47	.2394
390	4.021	143.45	.2447	3.707	143.44	.2439	3.439	143.41	.2430	3.005	143.36	.2416
400	4.069	145.34	0.2469	3.752	145.33	0.2461	3.481	145.31	0.2453	3.042	145.26	0.2438
410	4.117	147.25	0.2491	3.797	147.24	.2483	3.522	147.22	.2475	3.079	147.17	.2460
420	....	....	....	3.841	149.16	0.2505	3.562	149.14	0.2497	3.115	149.10	.2482
430	....	....	....	....	....	....	....	....	....	3.152	151.03	0.2504

TABLE 70 . . . PROPERTIES OF SUPERHEATED VAPOR (continued)

Temp F	Abs. Pressure 18 psi Gage Pressure 3.3 psi (Sat'n Temp 128.6 F)			Abs Pressure 20 psi Gage Pressure 5.3 psi (Sat'n Temp 134.6 F)			Abs Pressure 25 psi Gage Pressure 10.3 psi (Sat'n Temp 147.8 F)			Abs Pressure 30 psi Gage Pressure 15.3 psi (Sat'n Temp 159.1 F)		
t	v	h	s	v	h	s	v	h	s	v	h	s
(Sat'n)	(1.795)	(97.68)	(0.1764)	(1.625)	(98.56)	(0.1769)	(1.317)	(100.50)	(0.1778)	(1.109)	(102.15)	(0.1787)
130	1.799	97.91	0.1769	....	....	....	....	....	....	....	....	....
140	1.833	99.51	.1795	1.640	99.43	0.1783	....	....	....	....	....	....
150	1.867	101.12	0.1822	1.672	101.05	0.1810	1.322	100.87	0.1784	....	....	....
160	1.901	102.75	.1848	1.703	102.68	.1836	1.348	102.50	.1811	1.111	102.31	0.1790
170	1.935	104.39	.1675	1.734	104.32	.1862	1.373	104.14	.1837	1.132	103.96	.1816
180	1.968	106.04	.1901	1.765	105.97	.1888	1.398	105.80	.1863	1.153	105.62	.1842
190	2.002	107.71	.1926	1.796	107.64	.1914	1.423	107.47	.1889	1.173	107.29	.1868
200	2.036	109.39	0.1952	1.827	109.32	0.1940	1.448	109.15	0.1915	1.194	108.97	0.1894
210	2.069	111.08	.1977	1.857	111.01	.1966	1.472	110.84	.1940	1.215	110.67	.1919
220	2.103	112.77	.2003	1.887	112.70	.1991	1.497	112.54	.1966	1.236	112.37	.1945
230	2.136	114.47	.2028	1.917	114.40	.2016	1.522	114.25	.1991	1.257	114.03	.1970
240	2.169	116.18	.2052	1.947	116.12	.2041	1.546	115.96	.2015	1.278	115.80	.1995
250	2.203	117.90	0.2077	1.977	117.84	0.2065	1.571	117.69	0.2040	1.299	117.53	0.2019
260	2.236	119.64	.2101	2.007	119.58	.2090	1.595	119.44	.2064	1.320	119.28	.2044
270	2.269	121.39	.2125	2.037	121.33	.2114	1.619	121.19	.2089	1.341	121.03	.2068
280	2.303	123.15	.2149	2.068	123.09	.2138	1.643	122.95	.2113	1.362	122.60	.2092
290	2.336	124.92	.2173	2.098	124.87	.2162	1.667	124.73	.2137	1.382	124.59	.2116
300	2.370	126.72	0.2197	2.128	126.67	0.2185	1.691	126.53	0.2160	1.402	126.39	0.2140
310	2.403	128.53	.2220	2.158	128.47	.2209	1.716	128.34	.2184	1.422	128.20	.2163
320	2.436	130.34	.2244	2.187	130.28	.2232	1.741	130.16	.2207	1.442	130.02	.2187
330	2.469	132.16	.2267	2.217	132.10	.2255	1.765	131.98	.2231	1.462	131.85	.2210
340	2.502	133.99	.2290	2.247	133.94	.2278	1.789	133.82	.2254	1.483	133.69	.2233
350	2.535	135.83	0.2313	2.277	135.78	0.2301	1.813	135.66	0.2277	1.503	135.54	0.2256
360	2.569	137.69	.2336	2.308	137.64	.2324	1.838	137.52	.2300	1.524	137.40	.2279
370	2.602	139.55	.2358	2.338	139.50	.2347	1.862	139.39	.2322	1.545	139.27	.2302
380	2.635	141.43	.2381	2.368	141.38	.2369	1.886	141.26	.2345	1.565	141.15	.2324
390	2.667	143.32	.2403	2.398	143.27	.2392	1.910	143.15	.2367	1.585	143.05	.2347
400	2.700	145.22	0.2425	2.427	145.17	0.2414	1.933	145.05	0.2389	1.604	144.95	0.2369
410	2.733	147.13	.2447	2.456	147.08	.2436	1.957	146.97	.2411	1.624	146.86	.2391
420	2.765	149.05	.2469	2.485	149.01	.2458	1.981	148.90	.2433	1.645	148.79	.2413
430	2.797	150.99	0.2491	2.515	150.94	.2480	2.005	150.83	.2455	1.665	150.73	.2435
440	....	....	....	2.544	152.89	0.2501	2.029	152.78	.2477	1.685	152.68	.2457
450	....	....	....	....	....	....	2.052	154.74	0.2498	1.706	154.65	0.2479

Temp F	Abs Pressure 35 psi Gage Pressure 20.3 psi (Sat'n Temp 169.0 F)			Abs Pressure 40 psi Gage Pressure 25.3 psi (Sat'n Temp 177.9 F)			Abs Pressure 50 psi Gage Pressure 35.3 psi (Sat'n Temp 193.5 F)			Abs Pressure 60 psi Gage Pressure 45.3 psi (Sat'n Temp 206.9 F)		
(Sat'n)	(0.9580)	(103.60)	(0.1795)	(0.8435)	(104.90)	(0.1802)	(0.6809)	(107.14)	(0.1816)	(0.5705)	(190.06)	(0.1827)
170	0.9594	103.77	0.1797	....	....	....	....	....	....	....	....	....
180	0.9780	105.43	.1824	0.8462	105.26	0.1808	....	....	....	....	....	....
190	0.9963	107.10	.1850	0.8627	106.94	.1834	....	....	....	....	....	....
200	1.015	108.79	0.1876	0.8791	108.62	0.1860	0.6899	108.27	0.1833	....	....	....
210	1.033	110.49	.1901	0.8953	110.32	.1885	0.7031	109.97	.1858	0.5738	109.60	0.1835
220	1.051	112.20	.1927	0.9114	112.03	.1911	0.7163	111.69	.1884	.5853	111.31	.1861
230	1.069	113.91	.1952	0.9274	113.74	.1936	0.7296	113.41	.1909	.5968	113.04	.1886
240	1.088	115.63	.1977	0.9435	115.47	.1961	0.7430	115.14	.1934	.6082	114.78	.1912
250	1.106	117.37	0.2002	0.9596	117.21	0.1986	0.7562	116.90	0.1959	0.6193	116.54	0.1937
260	1.124	119.12	.2026	0.9756	118.97	.2010	0.7693	118.67	.1984	.6303	118.32	.1961
270	1.142	120.88	.2051	0.9915	120.74	.2035	0.7821	120.45	.2008	.6413	120.11	.1986
280	1.160	122.66	.2075	1.008	122.52	.2059	0.7950	122.23	.2033	.6525	121.91	.2010
290	1.177	124.45	.2099	1.023	124.31	.2083	0.8079	124.03	.2057	.6639	123.72	.2035
300	1.195	126.26	0.2122	1.038	126.12	0.2107	0.8207	125.84	0.2081	0.6751	125.53	0.2059
310	1.212	128.07	.2146	1.054	127.94	.2131	0.8335	127.66	.2104	.6860	127.36	.2083
320	1.230	129.89	.2169	1.070	129.76	.2154	0.8463	129.48	.2128	.6969	129.19	.2106
330	1.248	131.72	.2193	1.085	131.59	.2178	0.8591	131.31	.2152	.7079	131.03	.2130
340	1.266	133.56	.2216	1.101	133.44	.2201	0.8716	133.16	.2175	.7188	132.89	.2153
350	1.284	135.41	0.2239	1.117	135.29	0.2224	0.8844	135.02	0.2198	0.7296	134.75	0.2176
360	1.302	137.27	.2262	1.133	137.16	.2247	0.8973	136.89	.2221	.7403	136.63	.2199
370	1.319	139.15	.2285	1.148	139.03	.2269	0.9101	138.77	.2244	.7510	138.52	.2222
380	1.336	141.03	.2307	1.164	140.91	.2292	0.9228	140.67	.2266	.7619	140.42	.2245
390	1.353	142.93	.2329	1.179	142.81	.2314	0.9354	142.57	.2289	.7725	142.33	.2267
400	1.370	144.83	0.2352	1.194	144.72	0.2337	0.9480	144.48	0.2311	0.7831	144.24	0.2290
410	1.388	146.75	.2374	1.210	146.64	.2359	0.9605	146.41	.2333	.7937	146.16	.2312
420	1.405	148.68	.2396	1.225	148.57	.2381	0.9728	148.35	.2356	.8043	148.10	.2334
430	1.422	150.62	.2418	1.240	150.51	.2403	0.9851	150.30	.2378	.8151	150.06	.2356
440	1.439	152.58	.2440	1.256	152.47	.2425	0.9974	152.25	.2400	.8257	152.02	.2378
450	1.457	154.54	0.2461	1.271	154.44	0.2447	1.010	154.22	0.2421	0.8362	154.00	0.2400
460	1.474	156.52	.2483	1.286	156.41	.2468	1.023	156.21	.2443	.8466	155.98	.2422
470	1.491	158.51	0.2505	1.302	158.40	.2490	1.036	158.20	.2464	.8570	157.58	.2443
480	....	....	....	1.317	160.40	0.2511	1.048	160.20	.2486	.8675	159.98	.2465
490	....	....	....	....	....	....	1.060	162.22	0.2507	0.8776	162.00	0.2486

APPENDIX II

SAMPLES OF DATA PAGES

AND SAMPLE DATA

Sample Data Sheet

Date: May 11/72

B_a PR 736 in Hg @76°F

Room Temp: 83.5

Data Listing Page 5 Column 2

Run No. 4

Heater: 59

Riser Size: 58

Heater Elevation: 0

Heat Input Section Static Pressure Drop Correction for Zero (Inches of Freon)	15.5 -0.9 +.05	15.0 -0.8 +.05	
Mass Flow Reading Correction for Zero	7.1 - 3.8 - .05	7.25 - 3.95 - .05	
Heat Input Section Potentiometer Readings Bottom to Top (Millivolts) 1 Iron-Constantan 2 3 4 5 6 7 8	 2.907 2.758 2.7 2.514 2.425 2.271 2.231 2.231		
Potentiometer Readings Copper Constantan (Miilivolts) Heat Input Section Outlet Riser Section Inlet Three Feet Up Riser Heat Input Section Inlet	 2.377 2.367 2.362 1.750		
Power Upper Heater Volts x amps Lower Heater Volts x amps	 210 x 11.4 70 x 7.85	 212.5 x 11.5 70 x 7.85	 215 x 11.65 70 x 7.85
Flow Situation		Very near reversal	Reversal

Raw Data Partially Reduced

Date	June 29/72	May 30	May 30	May 31
Heater Length	59 inches	59	59	59
Heater Position	0 inches	2	6	21
Barometric Pressure	756.0mm @76°F	740.1 @73	740.1 @73	744.4 @67
Room Temperature	83.5°F	74.5	75	78.5
Test Section Pressure Drop	14.65 in Freon	14.6	14.9	14.50
Mass Flow Rate	.485 lbm/sec	.467	.467	.453
Inlet Temperature	110.0°F	109.2	109.4	108.8
Outlet Temperature	136.3°F	135.1	134.9	132.8
Total Power at Reversal	3054 watts	3044	2933	2497
Total Power Before Reversal	2943 watts	2923	2879	2447
HI Section Outlet Temperature	1350°F	135.1	134.9	132.8
Riser Section Inlet Temperature	134.6°F	134.8	134.5	132.5
Temperature 3 Feet Up Riser	134.1°F	134.1	133.9	132.1
Temperature In Heat Input Section Bottom to Top				
T1	132.2°f	133.2	131.7	129.8
T2	128.2°F	128.2	129.3	132.2
T3	125.8°F	126.2	127.8	132.7
T4	119.0°F	119.3	121.3	127.0
T5	116.3°F	116.5	118.3	124.3
T6	111.0°F	111.3	112.8	119.0
T7	108.8°F	108.7	108.3	113.5
T8	109.8°F	109.2	109.5	110.7
Page Number	5	5	6	7
Column Number	2	6	3	5

Sample of Final Data

Heater Length	Position inches	Page	Column	Flow Rate lbm/hr	X %
48"	-1	1	1	1710	6.72
	1	1	2	1692	6.68
	1	1	3	1681	6.85
	3	1	4	1681	6.69
	5	1	5	1681	6.75
	5	1	6	1674	6.55
	7	2	1	1674	6.44
	7	2	2	1674	6.50
	9	2	3	1681	6.48
	9	2	4	1674	6.39
	11	2	6	1638	6.36
	11	2	7	1656	6.36
	13	3	1	1674	6.21
	16	3	2	1656	6.14
	16	3	3	1595	6.30
	21	3	4	1620	5.79
	37	3	5	1595	4.72
				END	MAXIMUM
48"	1	4	1	1440	4.02
	5	4	2	1404	4.02
	9	4	3	1378	3.88
	9	4	4	1404	3.98
	13	4	5	1422	3.98
				END	MINIMUM
59"	-1	5	1	1692	6.84
	1	5	2	1746	6.95
	3	5	4	1681	6.66
	5	5	7	1681	6.76
	5	6	1	1681	6.88
	7	6	2	1692	6.69
	7	6	3	1681	6.82
	7	6	4	1674	6.69

Heater Length	Position inches	Page	Column	Flow Rate lbm/hr	X %
59"	9	6	5	1681	6.70
	9	6	6	1674	6.96
	11	6	7	1674	6.43
	11	7	1	1656	6.59
	13	7	2	1656	6.36
	13	7	3	1674	6.31
	18	7	4	1656	6.21
				END	MAXIMUM
59"	1	8	1	1422	3.98
	5	8	2	1422	3.93
	9	8	3	1422	3.98
	13	8	4	1422	4.01
				END	MINIMUM
22"	-2	9	1	1638	5.26
	0	9	2	1530	4.43
	0	9	3	1620	4.94
	2	9	4	1548	4.68
	4	9	5	1595	4.70
	6	9	6	1584	4.69
	6	9	7	1523	4.63
	10	10	1	1548	4.92
	10	10	2	1595	4.90
	12	10	3	1537	4.78
	17	10	4	1523	4.68
	20	10	5	1512	4.26
	25	10	6	1523	4.90
	30	10	7	1512	4.41
	30	11	1	1523	4.59
	40	11	2	1512	4.44
				END	MAXIMUM
22"	0	12	1	1440	3.82
	10	12	2	1422	4.02
	20	12	3	1440	3.95
	30	12	4	1440	4.01
	30	12	5	1422	3.96
	40	12	6	1422	3.96
				END	MINIMUM

Heater Length	Position inches	Page	Column	Flow Rate lbm/hr	X %
36"	1	13	1	1674	5.98
	11	13	2	1656	5.99
	21	13	3	1631	5.72
	37	13	4	1595	5.44
				END	MAXIMUM
36"	1	13	5	1422	3.91
	21	13	6	1386	4.02
	37	13	7	1440	4.09
				END.	MINIMUM
84"	1	14	1	1710	6.87
	5	14	2	1692	6.61
	5	14	3	1656	7.15
	5	14	4	1638	6.91
	5	14	5	1681	7.03
	11	14	6	1674	6.30
	11	14	7	1681	6.53
	21	15	1	1631	6.71
	37	15	2	1595	5.60
				END	MAXIMUM
	1	15	3	1386	3.87
	21	15	4	1386	4.01
	37	15	5	1404	4.05
				END	MINIMUM

REFERENCES

1. Gaspar, R., A Visual Study of Downflow Convection of a Two Phase Liquid, A Summer Project Report, Atomic Energy of Canada Limited (CRNL), Chalk River, Ontario (1968).
2. Carver, M.B., personal communication, (1968).
3. D'Arcy, D.F., personal communication, (1968).
4. Wikhammer, G.A., personal communication, (1968).
5. Groeneveld, D.C., personal communication, (1968).
6. Rogers, J.T., personal communication, (1969).
7. Barns, G.M., Cooling of a Vertical Nuclear Power Reactor at Low Powers by Thermosyphoning-induced Downflow, Canadian General Electric Company Technical Report, Nuclear Energy Project, (1969).
8. D'Arcy, D.F., personal communication, (1968).
9. Carver, M.B. and R. Gaspar, Experiments on Flow Instability in a Small Freon Loop, CRNL-199, Atomic Energy of Canada Limited, Chalk River, Ontario, (1968).
10. Carver, M.B., D.F. D'Arcy, G.A. Wikhammer, J.E. Casterline, and B. Matzner, Instabilities in Flow Through Multirod Bundles and Their Effect on Dryout, AECL-2716, Atomic Energy of Canada Limited, Chalk River, Ontario, (1968).
11. Forrest, A.R., Control and Instrumentation Practices, Sub Section 1 - Primary Flow Elements, Chalk River Nuclear Laboratories Engineering Manual, DE-13 (11.1), Chalk River, Ontario, (1964).
12. Chapman, A.J., Heat Transfer, 2nd Ed., pp. 363-368, pp. 382-385, The Macmillan Company, New York, (1967).
13. Kreith, F., Principles of Heat Transfer, 2nd Ed., pp. 434-469, International Textbook Company, Scranton, Pa., (1965).
14. Messersmith, C.W. and C.F. Warner, Mechanical Engineering Laboratory, pp. 36-39, John Wiley and Sons Inc., New York, (1950).

15. Neville, A.M. and J.B. Kennedy, Basic Statistical Methods for Engineers and Scientists, International Textbook Company, Scranton, Pa., (1964).

16. American Society of Heating, Refrigerating and Air-Conditioning Engineers, New York, ASHRAE Guide and Data Book Fundamentals and Equipment, pp. 281-292, pp. 320-323, (1965).

17. The Chemical Rubber Co., Handbook of Tables for Applied Engineering Science, pp. 48, 54, 681.

18. Simpson, L.L., Sizing Piping for Process Plants, Chemical Engineering, pp. 203-214, (June, 1968).

19. Bonilla, C.F., Nuclear Engineering Handbook, pp. 9.31-9.39 Sect. 4.4-4.6, McGraw Hill Book Company, Inc. (1958).

20. Pao, R.H.F., Fluid Dynamics, pp. 336-342, Charles E. Merrill Books, Inc., Columbus, Ohio, (1967).

21. Van Wylen, G.J. and R.E. Sonntag, Fundamentals of Classical Thermodynamics, John Wiley and Sons, Inc., New York, (1965).

22. Tong, L.S., Boiling Heat Transfer and Two Phase Flow, John Wiley and Sons, Inc., New York, (1966).

23. Gnyp, A.W. and C.C. St. Pierre, A Guide to Technical Writing, Department of Chemical Engineering, University of Windsor, Windsor, (1965).

VITA AUCTORIS

1946 Born in Windsor, Ontario on April 15

1965 Completed High School at Merlin District High School, Merlin, Ontario in June

1969 Received the Degree of Bachelor of Applied Science in Mechanical Engineering from the University of Windsor, Windsor, Ontario.